
Invited paper

The fine structure of marine hydrophysical fields and its influence on the behaviour of plankton: an overview of some experimental and theoretical investigations

OCEANOLOGIA, 45 (4), 2003.
pp. 517–555.

© 2003, by Institute of
Oceanology PAS.

KEYWORDS

Small-scale stratification
Intermittent stratification
Fine structure
Turbulence
Turbulent mixing
Turbulent diffusion
Phytoplankton
Zooplankton

CZESŁAW DRUET

Institute of Oceanology,
Polish Academy of Sciences,
Powstańców Warszawy 55, PL-81-712 Sopot, Poland;
e-mail: druet@iopan.gda.pl

Manuscript received 31 July 2003, reviewed 17 November 2003, accepted 20 November 2003.

Abstract

This article is an overview which presents in brief some of the results of research done in the last 20 years on the structure and dynamics of intermittent fine structure in the euphotic zone of the sea and its effect on the behaviour of marine plankton. The introduction provides a general characterisation of this structure and its relations with the plankton concentration field. Chapter 2 covers turbulent mixing processes in layers of homogeneous fine structure, and discusses the dynamic interactions of these layers and how these affect the behaviour of marine phyto- and zooplankton. The principal conclusions, in brief, are that the current state of knowledge, not only of intermittent fine structure itself and its dynamic transformations, but also of the influence of these processes on the behaviour of marine plankton, is today still a long way from permitting an accurate description of reality. Moreover, both empirical investigations (*in situ* and in the laboratory) and mathematical modelling, despite the quite advanced stage that the latter has reached, need to be continued. For this reason the prime aim of this article is to show up the gaps in our knowledge which future research in this complex, interdisciplinary area of oceanography should attempt to fill.

The complete text of the paper is available at <http://www.iopan.gda.pl/oceanologia/>

1. Introduction

Since the mid-1970s oceanographers and marine physicists have brought their intellectual and technical capabilities to bear on laboratory and *in situ* investigations of fine-scale variations in the structure of the hydrophysical fields of the ocean, both in time and in space. Following the implementation of increasingly accurate sensors and recording instruments to measure the thermal, salinity and dynamic states of the sea, it soon became clear that its hydrophysical fields are intermittently stratified in the vertical. Water layers displaying horizontal uniformity of flow velocity u , temperature T , salinity S , density ρ over a distance of several kilometres (Fig. 1) are by contrast homogeneous in the vertical over much shorter distances.

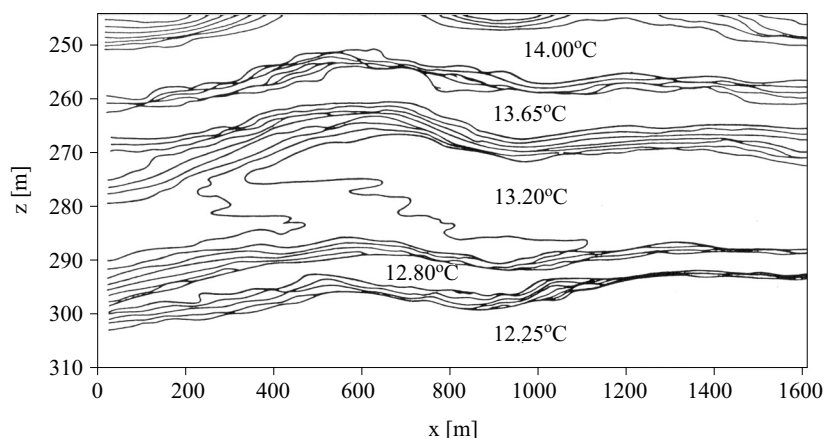


Fig. 1. An example of the fine structure of the temperature field (after Marmorino et al. 1987)

How long such intermittent stratification remains is not well known. The only assumption one can make is that this period is at least 10 minutes longer than the time interval separating two successive soundings. One should also recall that some of these structures can last up to a month, for example, in the tropical north-west Atlantic, or even a year, when the inhomogeneity has been created by a large-scale thermohaline circulation. The geometrical structure of these intermittent stratifications is such that vertically uniform or quasi-uniform layers c. 0.5–15 m thick are interspersed by very much thinner layers (c. 5–50 cm thick) with characteristically steep vertical gradients of the water's physical properties. This kind of vertical stratification has become known as 'fine structure' or 'small-scale stratification' (Gargett 1978, Monin & Ozmidov 1981, Ozmidov 1983, Žurbas & Lips 1987). The continuous vertical distribution of the physical

properties of the water ($\vartheta \equiv T, S, \rho, u$), recorded by a sufficiently sensitive meter at instant t_0 , can be divided into three component profiles (Fig. 2): $\vartheta(x, y, z, t_0) = \bar{\vartheta}(z) + \tilde{\vartheta}(z, t_0) + \vartheta'(x, y, z, t_0)$, where the $(-z)$ axis points downwards in accordance with the direction of action of the gravitational force. The $\bar{\vartheta}(z)$ profile reflects the classic, smooth vertical distribution of values averaged over a longer period of time, and is comparable with profiles obtained by means of point measurements. In the case of temperature, the measurement will have been performed with a reversible thermometer, and the salinity will have been determined by chemical analysis of water samples. The $\vartheta'(x, y, z, t_0)$ profile reflects the changes generated by micro-scale turbulence in the flow velocity field of the water masses (Gargett et al. 1984), while the $\tilde{\vartheta}(z, t_0)$ profile represents the fine structure.

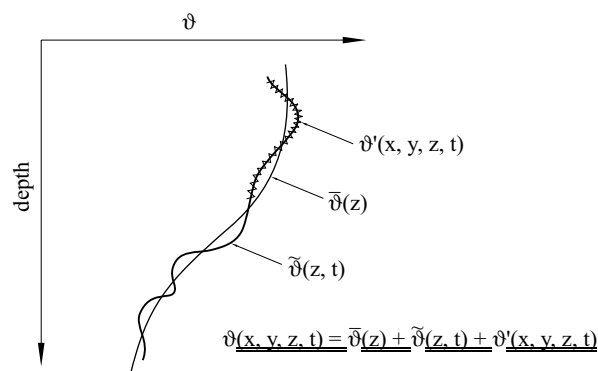


Fig. 2. Sensitive vertical profile of hydrophysical properties ($\vartheta \equiv T, S, \rho$), where $\bar{\vartheta}(z)$ – persistent mean profile, $\tilde{\vartheta}(z, t)$ – fine structure deviation, $\vartheta'(x, y, z, t)$ – small scale turbulence

The fine structure is shaped by the gravitational and inertial instability of the water masses and water flow, which generates turbulent mixing at depths where the laminar flow of the water, described by the Kelvin-Helmholtz equation, has been disturbed (inertial instability), or where there has been horizontal, intrusional interlayering of water masses differing from the surroundings in temperature and salinity (gravitational instability). In the latter case, mixing is caused either by thermal convection or by the formation of ‘salt fingers’. Medium- and large-scale gravitational instability leading to abyssal subsidence of water does not give rise to fine-scale vertical stratification. Using the simplest approach, we can distinguish three principal types of gravitational stability of water masses in the ocean:

- Absolute stability (Fig. 3), produced by the vertical temperature distribution decreasing with depth ($\partial \bar{T} / \partial z > 0$) and the salinity

distribution increasing with depth ($\partial\bar{S}/\partial z < 0$). These distributions cause an absolute increase in the mean density of the water with depth ($\partial\bar{\rho}/\partial z < 0$). Under such conditions, alternate homogeneous (mixed) layers can form only as a result of Kelvin-Helmholtz inertial instability.

- Relative stability (Fig. 4), produced by a vertical thermal inversion (unstable) ($\partial\bar{T}/\partial z < 0$) and stabilised by such a steep rise in salinity with depth ($\partial\bar{S}/\partial z \ll 0$) that the mean density of the water increases with depth ($\partial\bar{\rho}/\partial z < 0$). Given these conditions, intermittent homogeneous (mixed) layers form as a result of thermal convection processes.
- Relative stability (Fig. 5), produced by a vertical salinity inversion (unstable) ($\partial\bar{S}/\partial z > 0$), but which is so strongly stabilised by temperature decreasing with depth ($\partial\bar{T}/\partial z \gg 0$) that the mean density increases with depth ($\partial\bar{\rho}/\partial z < 0$). Under such conditions the alternate homogeneous layers come about through the formation of salt fingers.

Regardless of how these mixing processes are initiated, the dynamic characteristics of the fine structure are qualitatively almost identical in all three types of vertical stratification. That is to say, the homogeneous layers are more or less well mixed layers, while the flow of water in the

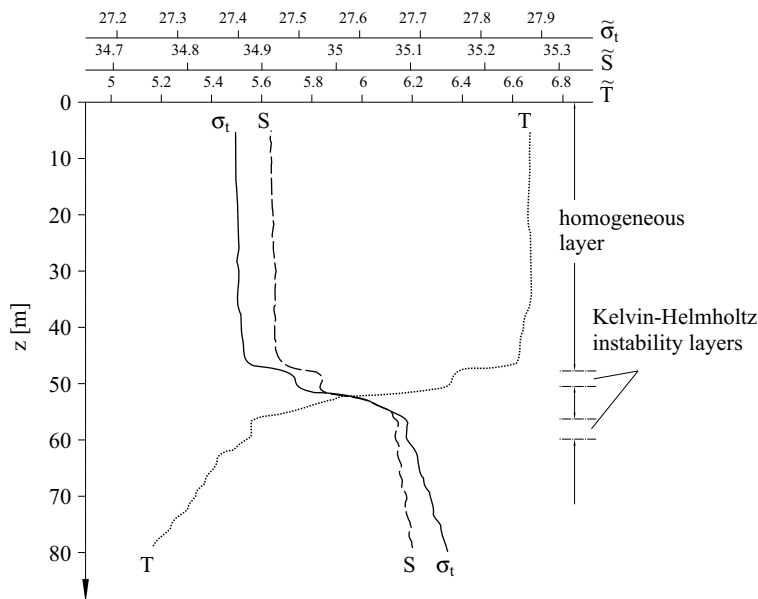


Fig. 3. Examples of the S , T , σ_t fine structure in stably stratified water masses (after Druet & Siwecki 1993) $\sigma_t = 10^3 [\rho(T, S) \rho(4.0)^{-1} - 1]$

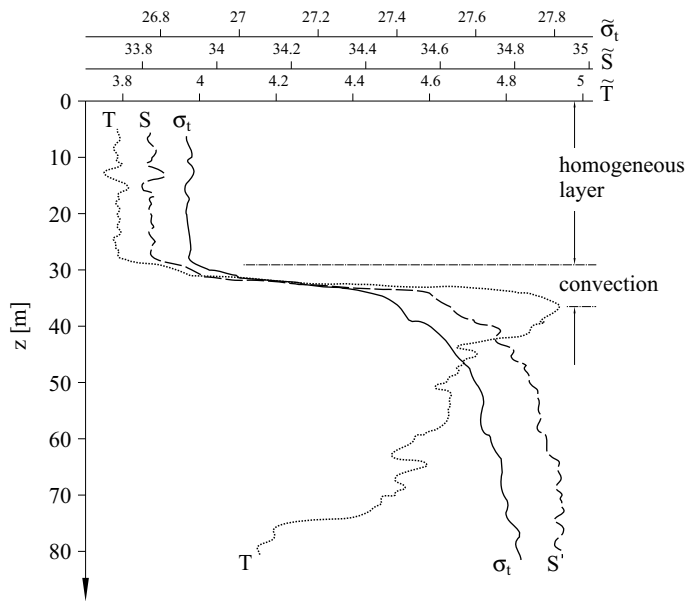


Fig. 4. Examples of the S, T, σ_t fine structure caused by thermal inversion (after Druet & Siwecki 1993) $\sigma_t = 10^3 [\rho(T, S) \rho(4.0)^{-1} - 1]$

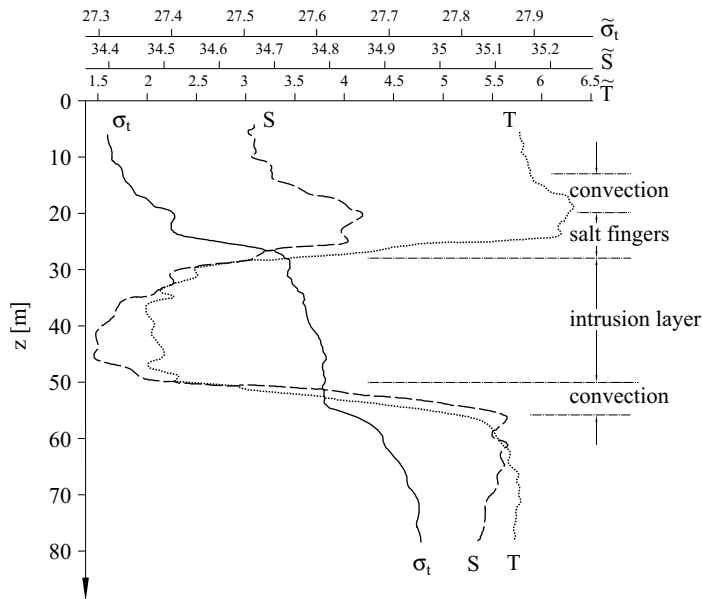


Fig. 5. Example of the S, T, σ_t fine structure caused by intrusion inflow (after Druet & Siwecki 1993) $\sigma_t = 10^3 [\rho(T, S) \rho(4.0)^{-1} - 1]$

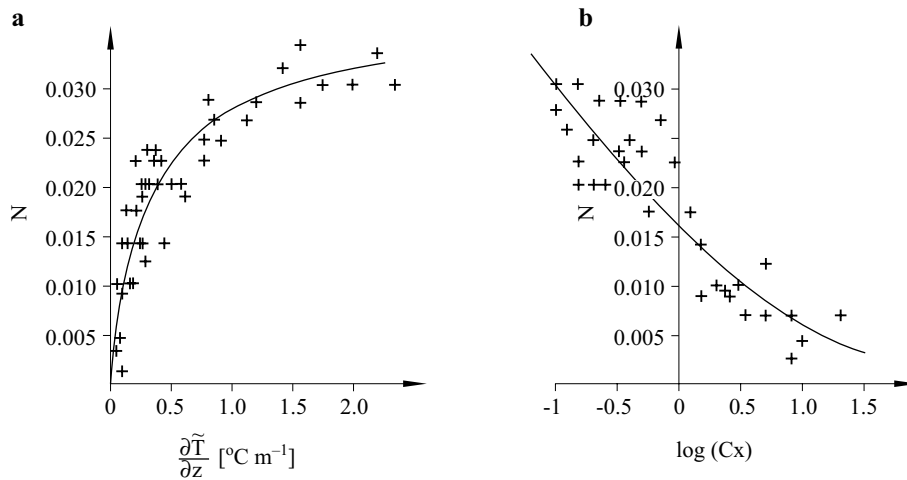


Fig. 6. Cox number Cx and vertical gradient of temperature fine structure ($\partial T/\partial z$) vs Väisälä-Brunt parameter N (after Druet & Siwecki 1985)

intervening thin, steeply-gradiented layers is, as a rule, laminar or quasi-laminar. If such an intermittent stratification of water masses endures for 15 minutes and more, it can be classified as fine structure. If on the other hand changes lasting a minute or less occur in the density field, such an unstable stratification is generated by the kinematic effect of internal waves, which is characterised by laminar flow and the absence of the mixing processes that give rise to fine structure. Examination of various aspects of fine structure in tideless seas like the Baltic or the Black Sea has shown that the effects of internal waves in the stable structure of the water density field are well illustrated by the functional dependence on the Väisälä-Brunt parameter N of a coefficient of turbulent mixing, e.g. the Cox number (Osborn & Cox 1972), and the vertical gradient of the fine-scale physical properties of water ($\partial \tilde{T}/\partial z$) (Fig. 6). It has also been discovered that under these conditions the mean height of internal waves, functionally associated with the standard deviation of fine-structural inhomogeneities, is also functionally dependent on the mean vertical gradient of the physical property in question (Fig. 7). Again, investigation of the random statistical properties of fine-scale structures has shown that the distributions of the function f of the probability that homogeneous layers of thickness b_0 occur can be approximated by the hyperbolic function (Fig. 8), where b_{\max} and b_{\min} are the largest and smallest thickness of a homogeneous layer in a statistically representative sample of random values of b_0 .

The few attempts at empirical *in situ* studies of the formation, development and disappearance of homogeneous layers have not yet yielded

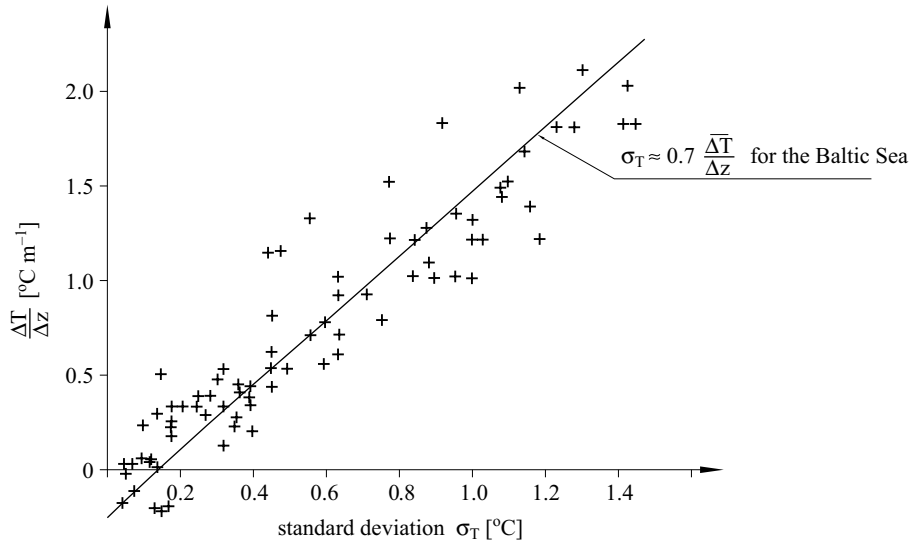


Fig. 7. Standard deviation σ_T of temperature fine structure vs mean temperature vertical gradient ($\overline{\Delta T}/\Delta z$) (after Druet & Siwecki 1985)

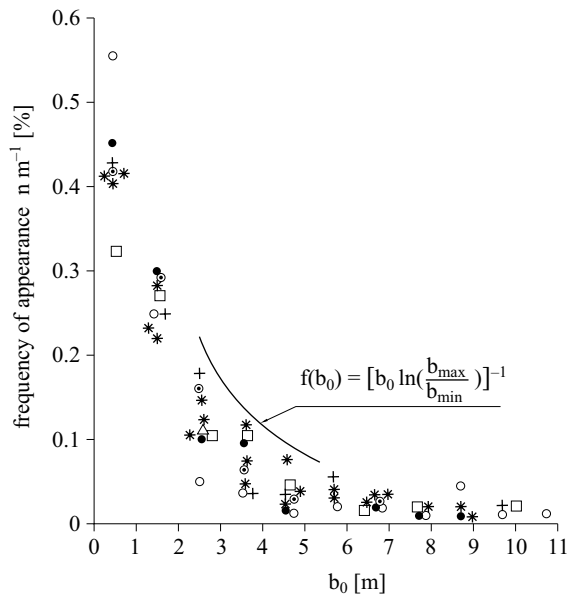


Fig. 8. Distribution of the empirical density function of probability $f(b_0)$ of the homogeneous layer thickness b_0 (after Druet & Siwecki 1985)

satisfactory results. However, the theoretical work of Lubimtzev (1985) on the development of an absolutely stable fine structure has led to a formula reflecting the evolution of a layer of thickness b_0 in a randomly intermittent stratification. In addition, the disappearance of fine structure, observed incidentally *in situ* over a period of six hours, merely showed (Fig. 9) that, with the passage of time, the layer of thickness b_0 gradually subdivided into thinner layers. This may herald the appearance in the structure of a larger number of thin, laminar or quasi-laminar gradential interlayers as the energy of the source of turbulent mixing dwindles.

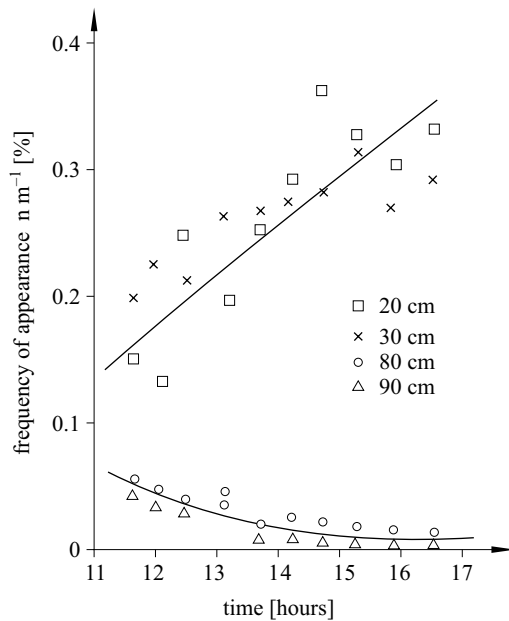


Fig. 9. Example of the rebuilding process of a homogeneous layer of thickness b_0 during storm decay (after Druet & Siwecki 1983)

Several results of *in situ* studies of the fine-scale structure of hydro-physical fields in the upper euphotic zone of the sea have shown that, outside storm periods, this zone too is characterised by an intermittent fine structure in which the turbulent homogeneous layers are from c. 15 to c. 50–60 cm thick, and the interspersed laminar layers are from c. 5 to c. 15 cm thick.

There is a conviction among oceanographers that this structure must necessarily affect the concentrations of diverse types of suspended matter, in particular the concentration fields of marine phyto- and zooplankton. The intensive, world-wide research effort of the 1980s and 1990s provided incontrovertible evidence that the individual growth of predatory organisms – from larval fish to herbivorous copepods – is linearly dependent on the

food concentration (phytoplankton, small zooplankton), which varies on a time-scale characterising the existence of fine structure (Davis et al. 1991). It was also demonstrated that the random movements of predators are negatively correlated with food concentration, so that they tend to stay longer in areas of higher concentrations, i.e. areas where their individual movements can be reduced to a minimum. In short, we can no longer investigate the environmental conditions governing the behaviour of plankton without taking account of the fact that their life processes are affected to a considerable extent by the turbulent mixing that homogenises the uniform fine structure layers. The behavioural sensitivity of larval fish and the larger zooplankton to local movements of the surrounding water masses are the more intensive, the lower their speeds of active movement in comparison with the speeds at which they are being carried along. A predatory member of the zooplankton, moving autonomously at speed v and capable of reacting to a food supply at distance R in time t will not sense the presence of turbulent eddies characterised by the linear orbital velocity of w_ω , unless $v > w_\omega$ and $R > v t$. The phytoplankton on the other hand, which is only capable of making slow vertical movements, is always going to experience nearby water movements and behave in turbulent eddies as a passive suspension. To recapitulate then, we can say that for all types of planktonic organism there are intervals of turbulent oscillations governing their aggregation, incubation and foraging processes. Figs 10 and 11 show the results obtained by Yamazaki & Squires (1996) and Peters & Marrase (2000), according to which zooplankton organisms up to 1 cm in size will

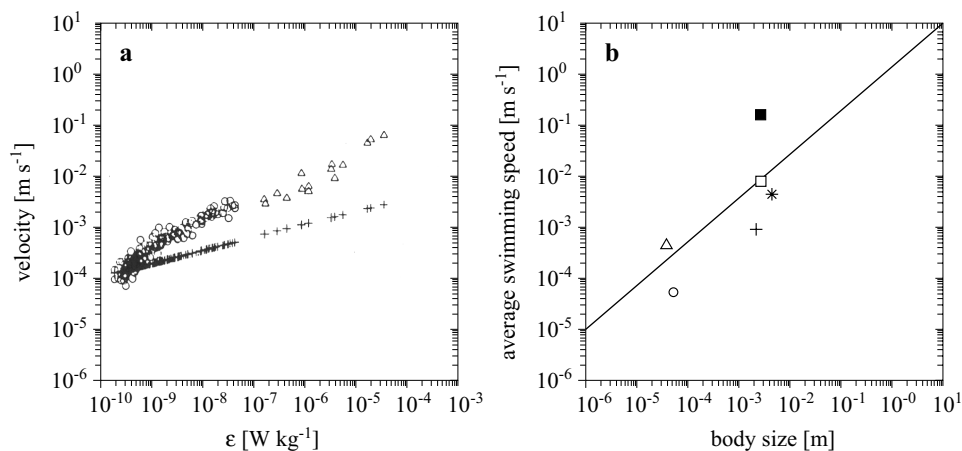


Fig. 10. a – Kolmogorov velocity scale (+) and the rms turbulent velocity scale vs observed dissipation rate ϵ ; b – average swimming speed vs body size of various organisms (after Yamazaki & Squires 1996)

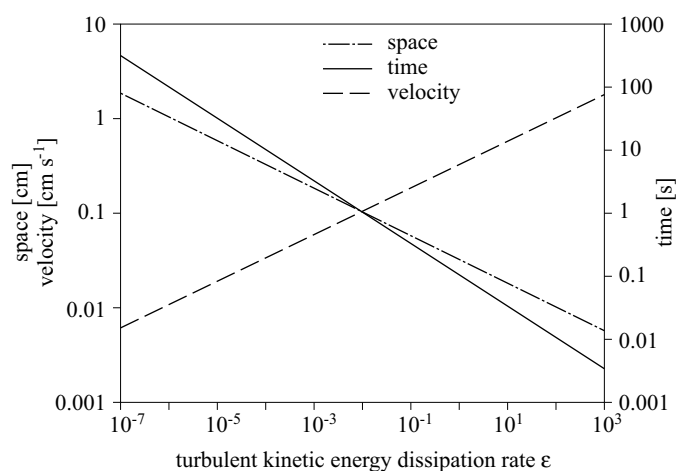


Fig. 11. Kolmogorov microscales against turbulence intensity (after Peters & Marrase 2000)

not react to turbulent eddies. Conversely, turbulent mixing in the inertial interval will affect organisms smaller than 1 cm, and the smaller they are, the greater the effect. The best example of this are the Copepoda. The plots in Fig. 10 also show that the rate of dissipation of turbulent eddy energy is quite a good indicator of the relation between the characteristics of plankton behaviour and those of turbulent mixing in a layer. Moderate turbulent mixing reduces the growth rate of individuals in that predators become homogenised, as it were, with their prey. But high-intensity turbulent mixing will cause the growth rate of predators to increase, especially among plankton displaying cruise-type behaviour (Dower et al. 1997), since there will be a rise in the encounter rate. Where mixing processes in a layer are weak, predators grow equally rapidly (Davis et al. 1991), especially among those that ambush their prey, because in such a layer the scattering of food concentrations is poor, and the attacker can forage more effectively.

The article further discusses selected results of empirical and theoretical investigations into the dynamics of turbulent interspersed layers and its influence on plankton behaviour in the euphotic zone. The point of this selective approach is to show up the gaps in our knowledge which future research in this complex, interdisciplinary area of oceanography should attempt to fill.

2. The dynamics of a fine-scale stratified sea

The theory of turbulent motion in water assumes that since a moving volume of water is very large in comparison with a water molecule, it is

possible to average the physical properties of the water in this volume, like temperature, passive admixture, density etc. At the same time, however, this volume should be sufficiently small in relation to the set of analogous volumes in the surroundings if mathematical modelling of the phenomenon is to be based on differential equations. This assumption, however, does not define the actual dimensions of this volume, so that in fact any magnitudes are acceptable, from millimetres in the modelling of fine-scale eddies to metres and larger in the case of medium- and large-scale oceanic flows. If we therefore take into consideration the linear scales of hydrodynamic processes, comparable with the dimensions of marine plankton ranging in size from phytoplankton to the larger zooplankton and larval fish, we can to a satisfactory approximation take the elementary volumes of moving water to be of the order of 1 mm^3 to 1 cm^3 . It is within this range of linear scales that the mathematical model of turbulent motion formulated by Reynolds in 1894 finds complete application. In accordance with this theory, the slow motion of elementary volumes of water, which form a horizontal laminar stream of water in which only the water molecules change position, is destroyed at the instant the acceleration of a stream of elementary water volumes causes these to move from the maternal stream to a neighbouring one. In a gravitationally absolutely stable marine basin, in which $(\partial \bar{T} / \partial z > 0)$, $(\partial \bar{S} / \partial z < 0)$ and $(\partial \bar{p} / \partial z < 0)$, this instant defines the stability condition of the Kelvin-Helmholtz equation (Stern 1975):

$$N^2(z) > 0.25 \left(\frac{\partial \bar{u}}{\partial z} \right)^2 . \quad (1)$$

$N(z) = \left(\frac{g}{\rho} \frac{\partial \bar{p}}{\partial z} \right)^{1/2}$ is the Väisälä-Brunt parameter and \bar{u} is the mean velocity of a horizontal flow. This expression contains a magnitude known as the gradiental Richardson number: $Ri = N^2 \left(\frac{\partial \bar{u}}{\partial z} \right)^{-2}$. Using Ri , we see that inertial instability (turbulent mixing) is initiated when $Ri < 0.25$. To express the efficiency of turbulence with respect to the work of buoyancy forces (Turner 1973) this condition is often expressed by the Richardson flux number R_f . Different researchers define R_f in various ways, one being to express it by means of the Froude number Fr (Ivey & Imberger 1991):

$$R_f = [1 + 3 Fr^2]^{-1} \quad \text{for} \quad Fr > 1.2, \quad (2)$$

where the Froude number $Fr = \left(\frac{\varepsilon}{\nu N^2} \right)^{1/2}$, ε is the measure of the rate of dissipation of the turbulent kinetic energy of the flow (the magnitude of ε is given later in this article), and ν is the kinematic coefficient of the molecular exchange of momentum (viscosity). Fig. 12 shows a plot of this relationship for turbulent fluctuations of water temperature. In the literature one can

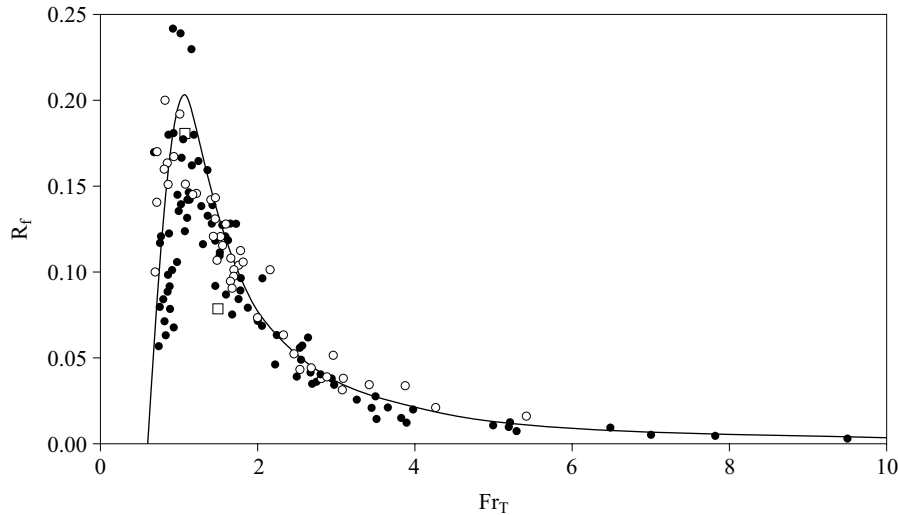


Fig. 12. Flux Richardson number R_f versus Froude number Fr_T (after Ivey & Imberger 1991)

also come across the relationship between the Richardson number and the kinetic energy alone E_k of turbulent fluctuations (Axell 2002):

$$Ri = E_k^2 \varepsilon^{-2} N^2,$$

where $E_k \approx \frac{1}{2} \langle (u')^2 + (v')^2 + (w')^2 \rangle$, u' , v' and w' are the components of turbulent fluctuations of flow, and the symbol $\langle \dots \rangle$ indicates spatial averaging.

Where the water masses are relatively stable and there is a temperature inversion ($\partial \bar{T} / \partial z < 0$, $\partial \bar{S} / \partial z \ll 0$, $\partial \bar{\rho} / \partial z < 0$), a homogeneous mixed layer begins to form when the Rayleigh number Ra exceeds the critical value:

$$(Ra)_{cr} = \frac{g \alpha \overline{\Delta T} H_k^3}{k_T \nu} > \frac{27}{4} \pi^4, \quad (3)$$

where the thickness of the mixed layer $H_k = \frac{27 \pi^4 k_T \nu}{g \alpha \overline{\Delta T}}$, $\alpha = \frac{1}{\rho} \frac{\partial \rho}{\partial T}$, $\overline{\Delta T}$ is the temperature difference at the boundaries of the mixed layers, and k_T represents the kinematic coefficient of molecular heat exchange.

In conditions satisfying this expression gravitational instability is generated by the convective motion of free elementary volumes of water. Dividing expression Ra by the Prandtl number $Pr = \frac{\nu}{k_T}$ we obtain the Grashof number Gr , which is frequently applied in estimates of convective mixing.

$$Gr = Ra Pr^{-1} = \frac{g \alpha \overline{\Delta T} H_k^3}{\nu^2}, \quad (4)$$

and the critical value of the temperature difference can be determined from the formula:

$$(\overline{\Delta T})_{cr} = \frac{27}{4} \pi \left(\frac{k_T \nu}{g \alpha H_k^3} \right). \quad (5)$$

When the water masses are relatively stable, and there is a salinity inversion ($\partial \overline{S}/\partial z > 0$, $\partial \overline{T}/\partial z \gg 0$, $\partial \overline{\rho}/\partial z < 0$), we have a situation in which differential diffusion takes place, and the homogeneous layer forms as a result of the vertical downward transport of both heat and salt in the form of 'salt fingers'. The criterion for the occurrence of this process in the water can be defined in the form of a stability parameter:

$$R_\rho = \frac{\alpha \overline{\Delta T}}{\beta \overline{\Delta S}}. \quad (6)$$

According to Schmitt (1979), the 'salt finger' process occurs within the following interval of R_ρ values:

$$1 < R_\rho < \frac{k_T}{k_S}, \quad (7)$$

where k_S is the kinematic coefficient of the molecular diffusion of salt.

The thickness of a fully developed homogenous layer is given by the length of the salt fingers (Gargett & Schmitt 1982):

$$b_0 = \frac{g \alpha \overline{\Delta T}}{\nu k_T k^4}, \quad (8)$$

where $k = \left[g \left(\alpha \frac{\partial \overline{T}}{\partial z} + \beta \frac{\partial \overline{S}}{\partial z} \right) (k_T \nu)^{-1} \right]^{1/4}$, $\beta = \frac{1}{\rho} \frac{\partial \rho}{\partial s}$.

One of the several practical methods of identifying the source of mixing processes in sea water is the graphical method based on the Turner angle Tu (McDougall et al. 1988):

$$Tu = \arctan \left[\frac{z \frac{\partial T}{\partial z} - \beta \frac{\partial s}{\partial z}}{\alpha \frac{\partial T}{\partial z} + \beta \frac{\partial s}{\partial z}} \right]. \quad (9)$$

Fig. 13 shows a diagram based on this formula enabling the source of the mixing process giving rise to the formation of fine-structured, homogenous layers to be identified. In an absolutely stable area this source can only be due to the Kelvin-Helmholtz inertial instability.

The inertial forces P_J generating and maintaining turbulent mixing are opposed by the forces of molecular and turbulent friction τ and of the buoyancy forces P_ρ in that the work of both these forces is directed against that of the inertial forces generating turbulent mixing. When these forces are in equilibrium, i.e. $P_J = P_\rho$, the linear scales of turbulent eddies take the form proposed by Ozmidov (1965):

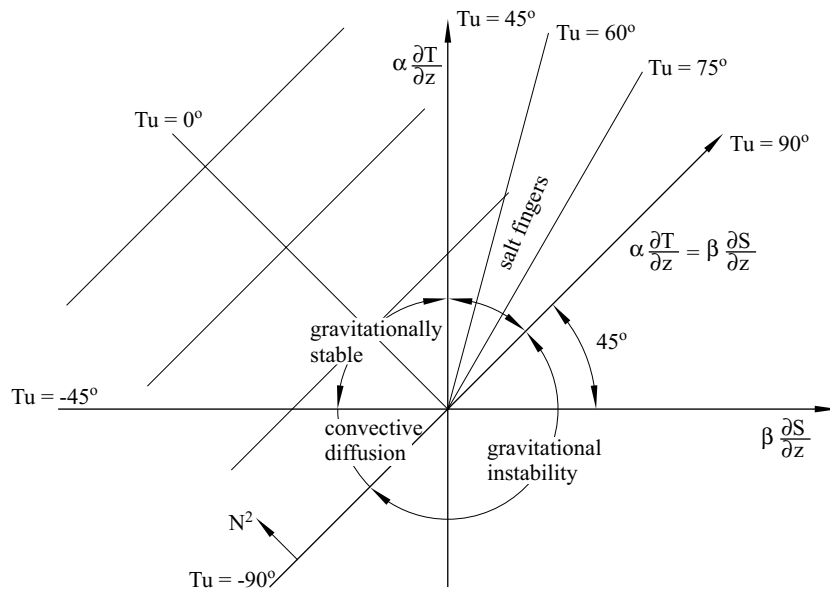


Fig. 13. A diagram based on the Turner angle 3.12 (after McDougall et al. 1988)

$$\ell_0 = (\varepsilon N^{-3})^{1/2}. \tag{10}$$

But the scales of turbulent eddies in existence when the influence of density upthrust forces is greater were expressed by Baumert & Peters (2000) in the form:

$$\ell_B = E_k^{1/2} N^{-1}, \tag{11}$$

where the quantity of E_k is a measure of the turbulent kinetic energy. Under conditions when turbulent fluctuations are completely damped by the buoyancy forces, $E_k = 0$ and $\ell_B = 0$.

The second, extreme case where turbulent mixing is damped is the one in which the inertial forces P_J balance the forces of molecular friction τ . The scales of turbulent eddies existing under such conditions were formulated by Kolmogorov (1962) thus:

$$\eta = q \left(\frac{\nu^3}{\varepsilon} \right)^{1/4}, \tag{12}$$

where q is a numerical coefficient of the order of unity.

The Reynolds condition of turbulent motion is a small-scale process and provides for a cascade mechanism according to which larger eddies generate smaller ones so that the kinetic energy of the former goes to produce the latter. In the literature this mechanism is known as the ‘Kolmogorov cascade’. Within this mechanism, the smaller eddies ‘live off’, as it were, the

energy of the larger eddies. By contrast, the largest eddies, of dimensions L_1 , are generated by an external energy source (wind, planetary motion, movements of the Earth's crust, etc.). The dimension L_1 sets the external limit to the turbulent cascade, the dimension η the internal limit, thus:

$$L_1 \geq \ell \geq \eta. \quad (13)$$

The cascade mechanism will remain in equilibrium, so long as the senses of all the vectors involved are balanced. In this case the turbulence is isotropic, and the rate of kinetic energy transfer from the larger to the smaller structures is a measure of the energy losses sustained by the turbulent energising eddies. This has been named the 'rate of dissipation of turbulent kinetic energy', and is usually defined by the formula:

$$\varepsilon = \beta_0^{-3} w_\omega^3 \ell^{-1}, \quad (14)$$

where w_ω is the linear orbital velocity of a turbulent eddy, and the linear scale of the eddy.

Hence the linear velocity of the orbital motion of elementary volumes of water in a turbulent cascade can be expressed as:

$$w_\omega = \beta_0 (\varepsilon \ell)^{1/3}. \quad (15)$$

The numerical coefficient β_0 in these expressions takes various values, depending on the interval:

- in the interval of the Kolmogorov scales ($\ell = \eta$): $\beta_0 \approx 1.9$ (Rothschild & Osborn 1988); for this interval Kolmogorov gave a different form of the equation:

$$w_\omega = (\varepsilon \nu)^{1/4}; \quad (16)$$

- in the interval of scales characterising inertial eddies: $\beta_0 \approx 1.37$ (MacKenzie & Kiørboe 2000).

Various publications quote different formulas expressing the rate of energy dissipation, and transform this expression by means of different parameters. For instance:

Osborn's (1980) formula for isotropic turbulence:

$$\bar{\varepsilon} = 7.5\nu \left(\frac{dw_\omega}{dz} \right)^2, \quad \text{or} \quad (17)$$

Gargett's (1997) formula:

$$\varepsilon = \gamma^2 N^3 \ell_{Th}^2, \quad (18)$$

where ℓ_{Th} is Thorpe's scale (Thorpe 1977, Dillon 1982), and the linear coefficient γ can take values in the interval $0.7 < \gamma^{1/2} < 1.4$.

In a three-dimensional, turbulent, locally isotropic cloud ($u' = v' = w'$) the mean rate of dissipation can be written as:

$$\bar{\varepsilon} = 15_1\nu \left(\frac{\partial u}{\partial z} \right)^2, \tag{19}$$

where u is the instantaneous velocity of the horizontal flow of water, and ν is the coefficient of molecular viscosity, or as:

$$\bar{\varepsilon} = 2\nu \int_0^\infty k^2 S(k) dk, \tag{20}$$

where $k = \frac{2\pi}{\ell}$ and $S(k)$ is the spectral function of turbulent fluctuations energy in the set of wave numbers k .

In the upper homogeneous layer of the sea, where the density is uniform (mixed), over which a wind blows with a speed of U_{10} , the mean rate of energy dissipation at depth ‘z’ can be expressed by the formula (Dower et al. 1997):

$$\bar{\varepsilon} = (5.82 \times 10^{-9}) \frac{U_{10}^3}{z}. \tag{21}$$

Table 1 gives some values of the parameters ε , η and $\partial u/\partial z$, Figs 14 and 15 give the example of a vertical distributions of \bar{T} , \bar{S} and $\bar{\varepsilon}$ in the upper layer of the North Atlantic at five points along a 12°E transect (Fig. 14) and four points along the Fårö-Shetland transect (Fig. 15).

Table 1. Values of parameters ε , η and $\partial u/\partial z$ (after Kiørboe & Saiz 1995)

Location	A. Typical values			B. Values in the upper layer			
	ε [cm ² s ⁻³]	η [mm]	$\partial \bar{u}/\partial z$ [s ⁻¹]	Wind speed [m s ⁻¹]	ε [cm ² s ⁻³]	η [mm]	$\partial \bar{u}/\partial z$ [s ⁻¹]
open ocean	10 ⁻⁶ –10 ⁻²	10–1.0	0.01–1	5	1.7 × 10 ⁻³	1.6	0.4
oceanic shelf	10 ⁻³ –10 ⁻²	1.8–1.0	0.32–1	10	1.5 × 10 ⁻²	0.9	1.2
shore zone	10 ⁻³ –10 ⁰	1.8–0.3	1–10	15	4.9 × 10 ⁻²	0.7	2.2
tidal front	10 ⁻¹	0.6	3.16	20	8.4 × 10 ⁻²	0.6	2.9

It is evident from the data given in this Table and on Figs 12 and 13 that the averaged rates of kinetic energy dissipation by turbulent eddy structures can vary within the range:

$$10^{-4} \geq \bar{\varepsilon} \geq 10^{-10} \text{ [m}^2 \text{ s}^{-3}\text{]}.$$

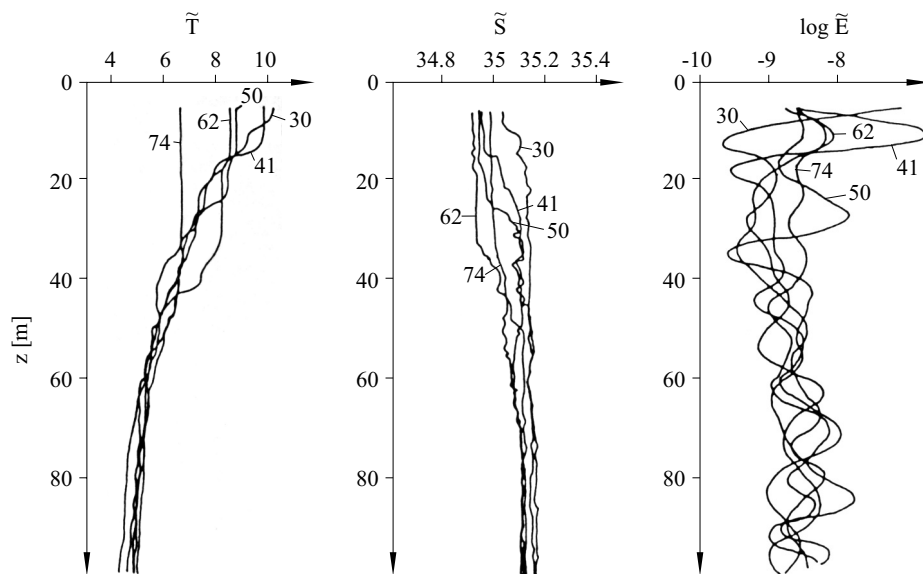


Fig. 14. Examples of the vertical fine structure profiles \tilde{T} , \tilde{S} , $\tilde{\epsilon}$ along a meridional transect 12°E of the North Atlantic Ocean (after Druet & Siwecki 1993)

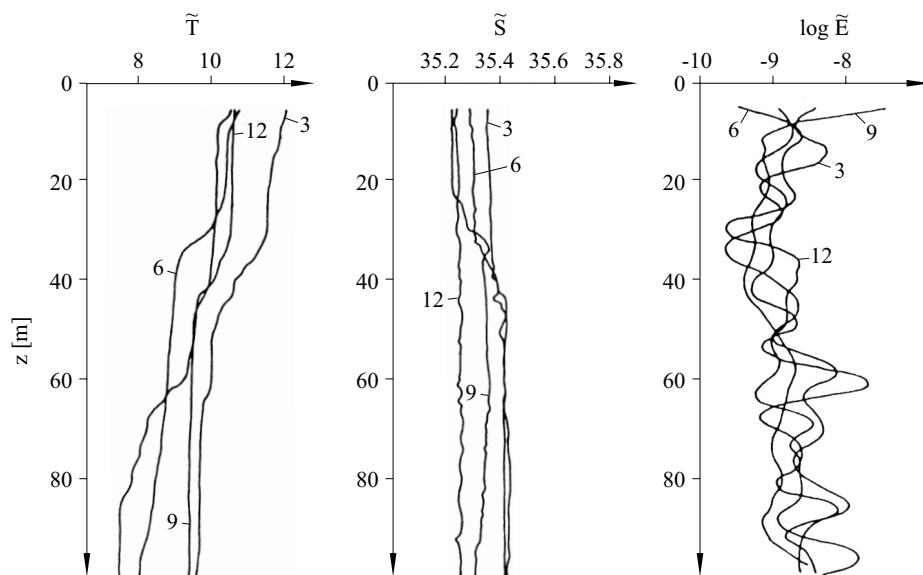


Fig. 15. Examples of the vertical fine-structure profiles \tilde{T} , \tilde{S} , $\tilde{\epsilon}$ along the Fårøe-Shetland transect (after Druet & Siwecki 1993)

The thickness of a turbulent cloud grows for as long as the process of hydrodynamic instability is supplied with energy, until the work done by inertial forces balances that of the forces of friction and buoyancy. This state is defined by the quantity $Ri \approx 0.4 \pm 0.1$ and is known as the Thorpe number (Garrett & Munk 1972): $Th \approx 0.4 \pm 0.1$. The thickness of the mixed layer in this balanced phase of development ($Ri \rightarrow Th$) is given by the formula (Garrett & Munk 1972):

$$b_{Th} \approx \frac{(\overline{\Delta u})_{Th}}{3.2\pi(N)_{Th}}, \tag{22}$$

where $(\overline{\Delta u})_{Th}$ is the difference in velocity at the upper and lower boundary of the layer, and $(N)_{Th}$ represents the Väisälä-Brunt frequency in the phase.

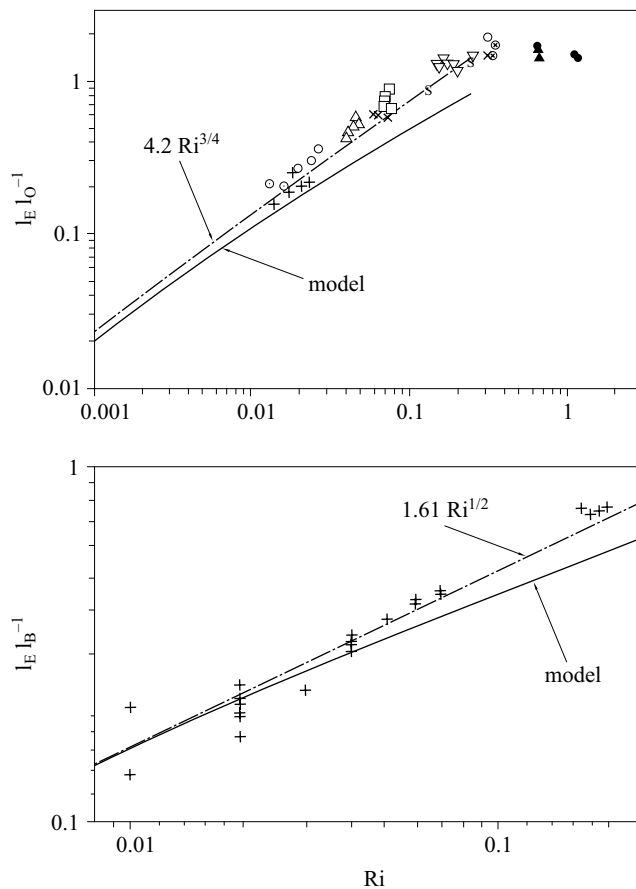


Fig. 16. Ratios of the Ellison scale ℓ_E to the Ozmidov scale ℓ_0 vs the Richardson number Ri and of the Ellison scale to the buoyancy scale ℓ_B vs the Richardson number (after Baumert & Peters 2000)

The rate of energy dissipation in turbulent mixing processes is a fundamental quantity. On the other hand, the Richardson number is also a good indicator of states of turbulent mixing. Since these states are defined by linear scales of turbulent rotation, their association with the Richardson number can be given by means of the relationship between the scales (Baumert & Peters 2000, Fig. 16):

$$\left. \begin{aligned} \frac{\ell_E}{\ell_0} \approx \frac{\ell_{Th}}{\ell_0} \approx 4.2 Ri^{3/4} \\ \frac{\ell_E}{\ell_B} \approx \frac{\ell_{Th}}{\ell_B} \approx 4.61 Ri^{1/2} \end{aligned} \right\} \text{ for } Ri > 0.25, \quad (23)$$

where ℓ_E is the Ellison scale, ℓ_0 is the Ozmidov scale ℓ_B is the buoyancy scale and ℓ_{Th} is the Thorpe scale.

Let us now consider the influence exerted by turbulent mixing processes in the intermittent fine structure on the behavioural states of marine plankton. The plots in Figs 17 and 18 show clearly the relationship between the concentration of suspended matter and the intensity of turbulent mixing: the more intense the turbulent mixing, the more widely dispersed the cloud of suspended matter and the lower its concentration. The upshot of this is obvious, and the highest concentration of phytoplankton is to be expected above or below thin laminar or quasi-laminar interlayers with steep density gradients. Investigations of greater precision usually involve mathematical modelling based on the equation of turbulent diffusion of phytoplankton and the nutrient supply to it (Druet & Zieliński 1988):

$$\left. \begin{aligned} \frac{\partial \bar{\vartheta}}{\partial t} + \frac{\partial}{\partial z}(\bar{w}_s \bar{\vartheta}) - \frac{\partial}{\partial z} \left[K(z) \frac{\partial \bar{\vartheta}}{\partial z} \right] - \Pi_1 \bar{\vartheta} = 0, \\ \frac{\partial \bar{N}_r}{\partial t} + \frac{\partial}{\partial z}(\bar{w}_s \bar{N}_r) - \frac{\partial}{\partial z} \left[K(z) \frac{\partial \bar{N}_r}{\partial z} \right] - \Pi_1 N_r = 0, \end{aligned} \right\} \quad (24)$$

where $\bar{\vartheta} = \bar{\vartheta}(z, t)$ is the horizontally averaged concentration of phytoplankton, $\bar{N}_r = \bar{N}_r(z, t)$ the averaged concentration of nutrients, and \bar{w}_s the averaged velocity of the vertical movement of phytoplankton. Π_1 is the function of the source of production and loss of concentration $\bar{\vartheta}$ and covers photosynthesis, mortality, respiration, as well as foraging by herbivorous zooplankton.

The fine structure dynamics are reflected in these eqs. by means of the coefficient of turbulent diffusion of a passive substance $K(z)$, on the assumption that vertically intermittent layers are horizontally homogeneous, i.e. $\partial/\partial x = \partial/\partial y = 0$. The problem of the analytical definition of the coefficient $K(z)$ has not yet been resolved and continues to be a research subject for hydrophysicists and oceanographers. The latter have attempted

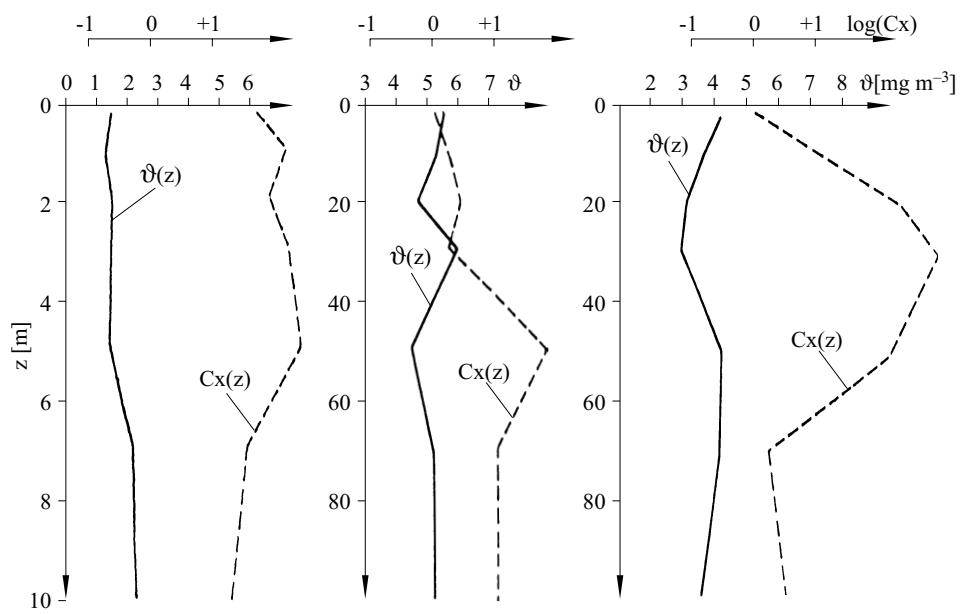


Fig. 17. Examples of the vertical distribution of the chlorophyll a concentration ϑ and Cox number Cx in the upper sea layer (after Druet & Zieliński 1988)

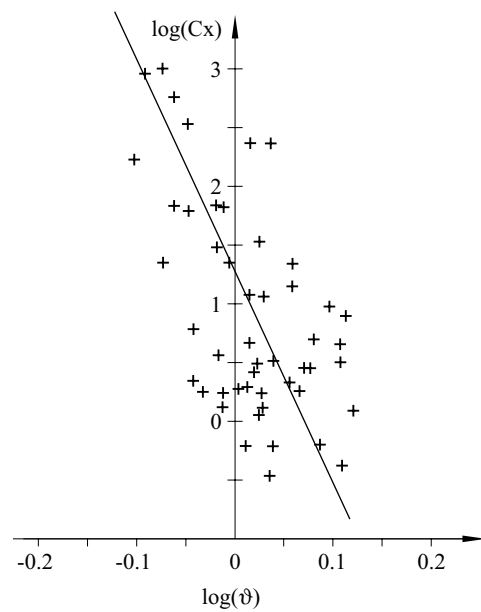


Fig. 18. Dependence of the chlorophyll a concentration ϑ on the Cox number Cx (after Druet & Siwecki 1985)

to find a formula for this coefficient not only empirically but also on the basis of the theory of similarity. In 1980 the fundamental form of coefficient $K(z)$ was formulated by Osborn:

$$K(z) = \Gamma \varepsilon N^{-2}(z), \tag{25}$$

where N is the Väisälä-Brunt parameter and Γ is an efficiency coefficient taking various values: according to Gregg (1989), $\Gamma \approx 0.2$, and according to Osborn himself (1980), Γ depends on the Richardson flux number and takes the form:

$$\Gamma = R_f(1 - R_f)^{-1}. \tag{26}$$

This formula in the interval of values $R_f \leq R_{f,max} \approx 0.15$ simplifies to the form $K(z) \leq 0.16 \varepsilon N^{-2}(z)$ (Itsweire et al. 1993). The values given in Table 2 give some idea of the variability of this relationship with respect to Ri .

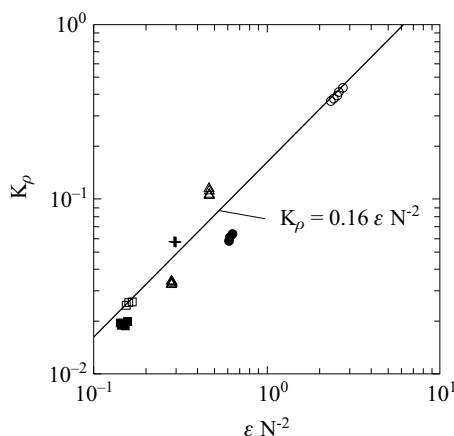
In 1998 Van Atta, analysing Osborn's formula, stated that Γ is equal to:

$$\Gamma = (1 + \gamma S_k) R_f(1 - R_f)^{-1}, \tag{27}$$

where the numerical coefficient γ is determined in quite a complex manner, and S_k stands for the kinetic energy of friction.

Table 2. Relations between the estimator of coefficient K and its real value, which is a function of Ri (after Itsweire et al. 1993)

Ri	$K(z) \leq 0.16 \varepsilon N^{-2}$
0.075	2.0
0.21	1.2
0.37	1.4



Other formulas worth mentioning include:

- the formula of Davis, Flierl, Wiebe and Franks (1991):

$$K(z) = 6.25 \times 10^{-3} \varepsilon(z), \tag{28}$$

- the formula of Peters, Gregg and Toole (1988):

$$K(z) = 5 \times 10^{-4} [1 + Ri(z)]^{-2.5} + 10^{-6}, \tag{29}$$

- the formula of Munk and Anderson (1948):

$$K(z) = K_0[1 + \beta_1 Ri(z)]^{-3/2}, \quad (30)$$

where $\beta_1 \approx 3.33$, $K_0 \approx 0.1$ (after Palegri & Csandy 1994, $K_0 \approx 2.6 \times 10^{-3} \text{ m}^2 \text{ s}^{-1}$),

- the formula of Pacanowski and Philander (1981):

$$K^T(z) = \{5 \times 10^{-3} + 10^{-4}[1 + 5Ri(z)]^2\}[1 + 5Ri(z)]^{-3} + 10^{-5}. \quad (31)$$

This last formula reflects the diffusion of heat, but a number of scientists are of the opinion that in turbulent motion heat is transferred together with mass, and that then one can assume that $K^T = K^\rho$. However, it should be mentioned in passing that Gibson (1987), the creator of the theory of fossil turbulence, disagrees fundamentally with this assumption. Nevertheless, if we do assume that $K^T = K^\rho$, Cox's empirical formula turns out to be useful in many cases (Osborn & Cox 1972):

$$K^T(z) = \left(\frac{\overline{\partial T'}}{\partial z}\right)^2 \left(\frac{\partial \overline{T}}{\partial z}\right)^{-2} k_T. \quad (32)$$

Unfortunately, though, this formula yields absurd values whenever the sign of the gradient of a physical property changes (Fig. 19). In 1988 Icha & Siwecki rewrote it as:

$$K^T(z) = 2 \left(\frac{\overline{\partial T'}}{\partial z}\right)^2 \left[2 \left(\frac{\partial \overline{T}}{\partial z}\right)^2 + K_z^\delta \frac{\partial^2}{\partial z^2} (\delta_T^2)\right]^{-1}, \quad (33)$$

where $\delta_T^2 = \overline{(T')^2}$ and $K_z^\delta = \alpha g \varepsilon_T^{-1/2} N^{-5/2} \ell^{-1}$.

The dependence of K on Ri for, $Ri > 0$, was studied by Large & Gent (1999), who formulated the coefficient of turbulent mixing in the following way:

$$K(z) = K_1 \left[1 - \frac{Ri(z)^2}{Ri_0}\right]^3 \quad \text{for } 0 < Ri < Ri_0. \quad (34)$$

The results of calculations given in Fig. 20 were obtained for $K_1 = 50 \times 10^{-4} \text{ m}^2 \text{ s}^{-1}$ and $Ri_0 = 0.7$ and $Ri_0 = 0.8$.

For the upper layer of a shallow sea, Lehfeldt & Bloss (1988) put forward an interesting proposition:

$$K(z) = \Psi \ell^2 \left(\frac{\partial \overline{u}}{\partial z}\right), \quad (35)$$

where $\Psi = (1 + Ri)^{-1}$, and the scale of turbulent structures $\ell = \ell(z) = 0.4H(1 + \lambda)\lambda^{1/4}$, $\lambda = \frac{|z|}{H}$, H is the depth of the basin in metres, and z is

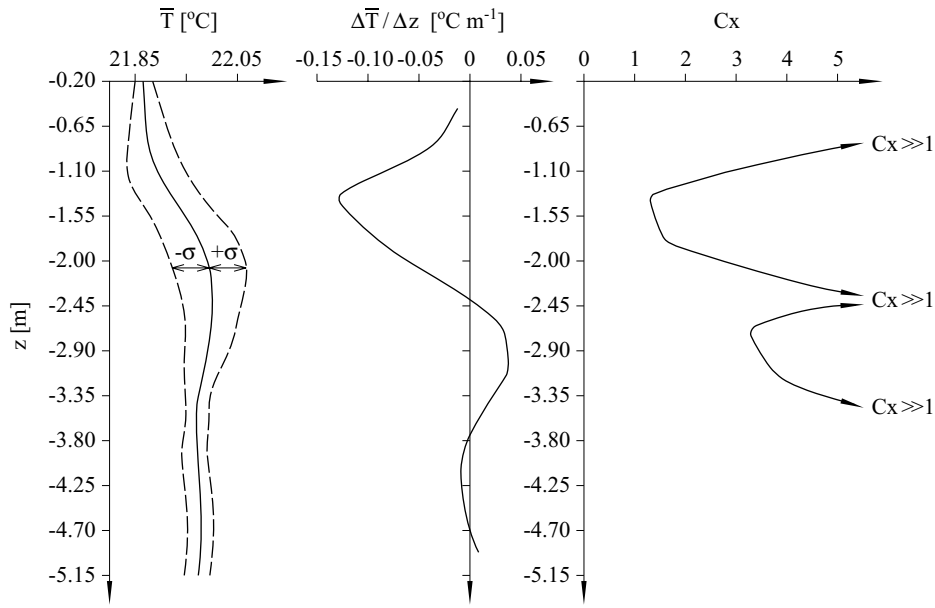


Fig. 19. Characteristics of the double thermocline and Cox number Cx in the presence of an off-shore wind (after Druet & Siwecki 1984)

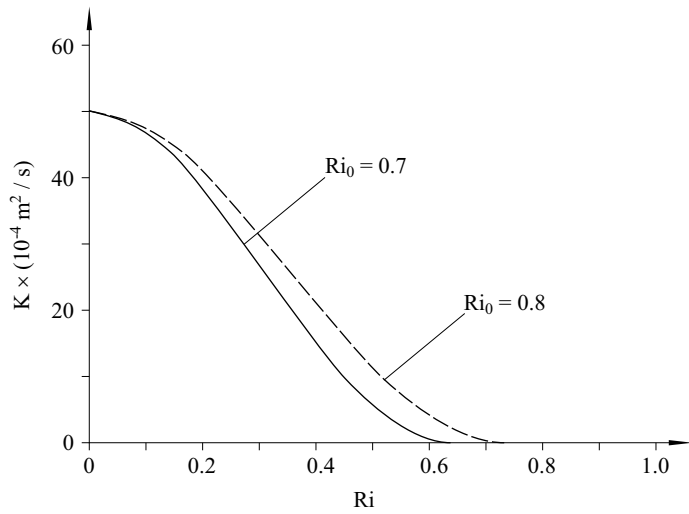


Fig. 20. Vertical diffusivity for shear instability mixing vs the Richardson number Ri for $Ri_0 = 0.7$ (solid line) and $Ri_0 = 0.8$ (dashed line) (after Large & Gent 1999)

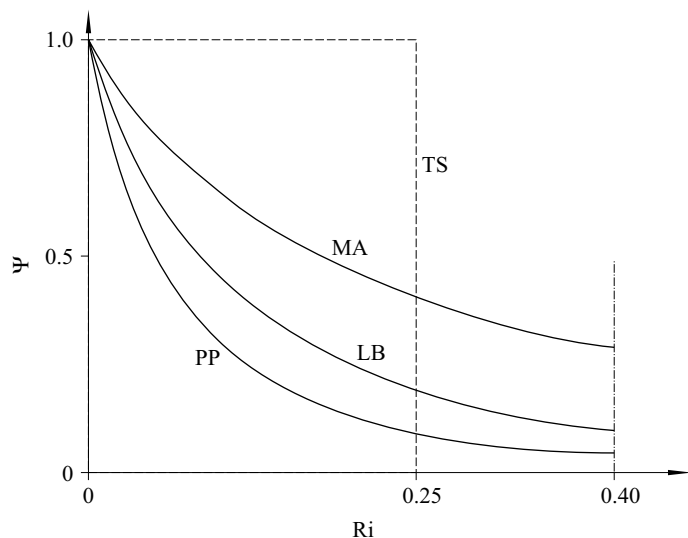


Fig. 21. Coefficient of mass diffusion vs the Richardson number Ri after: MA – Munk & Anderson (1948), TS – Thompson (1980), PP – Pacanowski & Philander (1981), LB – Lehfeldt & Bloss (1988) (after Nunes Vaz & Simpson 1994)

the distance from the free surface or bottom of the basin in metres. Fig. 21 shows comparative plots of a number of formulas compiled by Nunes Vaz & Simpson in 1994.

3. The effect of turbulent mixing on the marine plankton concentration field

The results of computer simulation studies based on equation 24 have shown (Figs 22, 23, 24) that the coefficient $K(z)$ representing turbulent mixing in the diffusion equations exerts a considerable influence on the state of phytoplankton concentration. Homogeneous layers are strongly dispersed with consequent thinning out of the suspended matter, which moves above the laminar gradiental interlayers, where it increases its concentration. One is entitled to pose the question, whether a phytoplankton concentration fine structure does indeed come into existence under natural conditions. The answer can be found either through *in situ* studies, or by performing simulations based on real vertical distributions of the water's hydrophysical properties. Such investigations have been carried out by Druet & Zieliński (1994) and Dzierzbicka (2000) on the basis of the system of turbulent diffusion equations, where background data for numerical modelling are shown in Fig. 25. The salinity distribution $S_0(z) = \text{const}$, and the

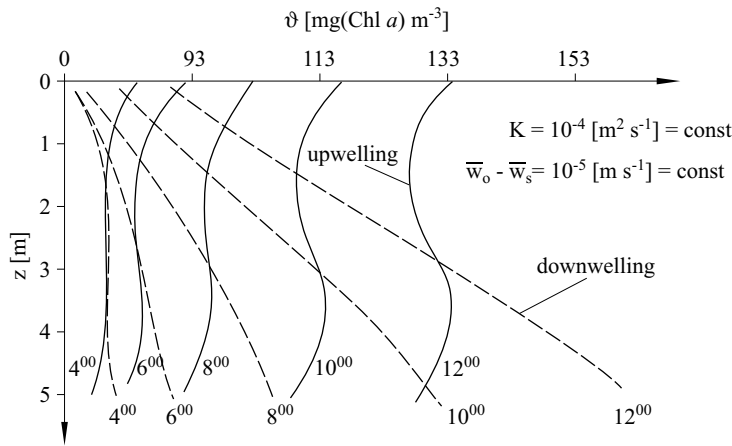


Fig. 22. Evolution in time (from 4:00 h to 12:00 h) of the vertical distributions of chlorophyll ϑ during upwelling and downwelling water flows; result of numerical modelling (after Druet & Zieliński 1988)

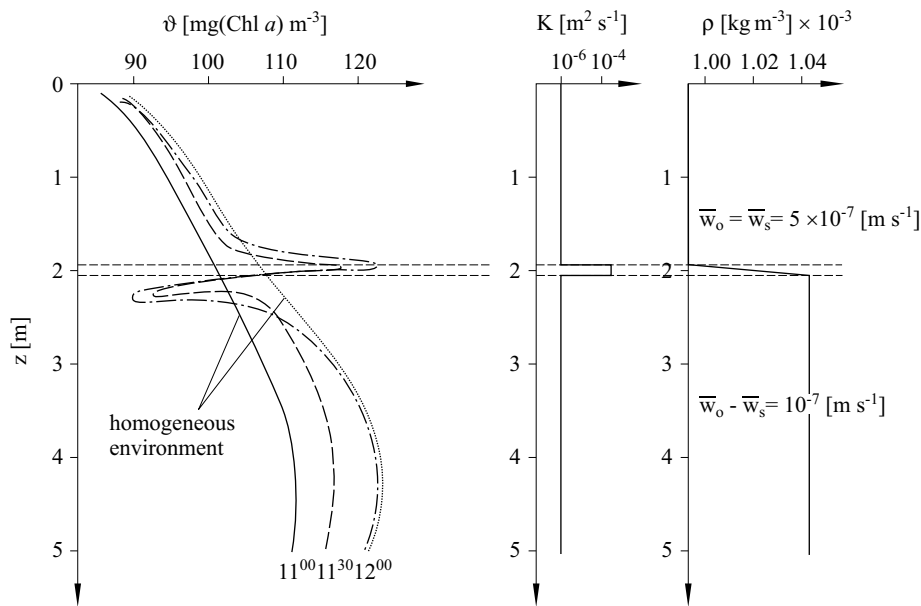


Fig. 23. Evolution in time of the vertical distributions of chlorophyll ϑ during plankton sinking and the presence of turbulent mixing in a 9 cm thin layer: results of numerical modelling (after Druet & Zieliński 1988)

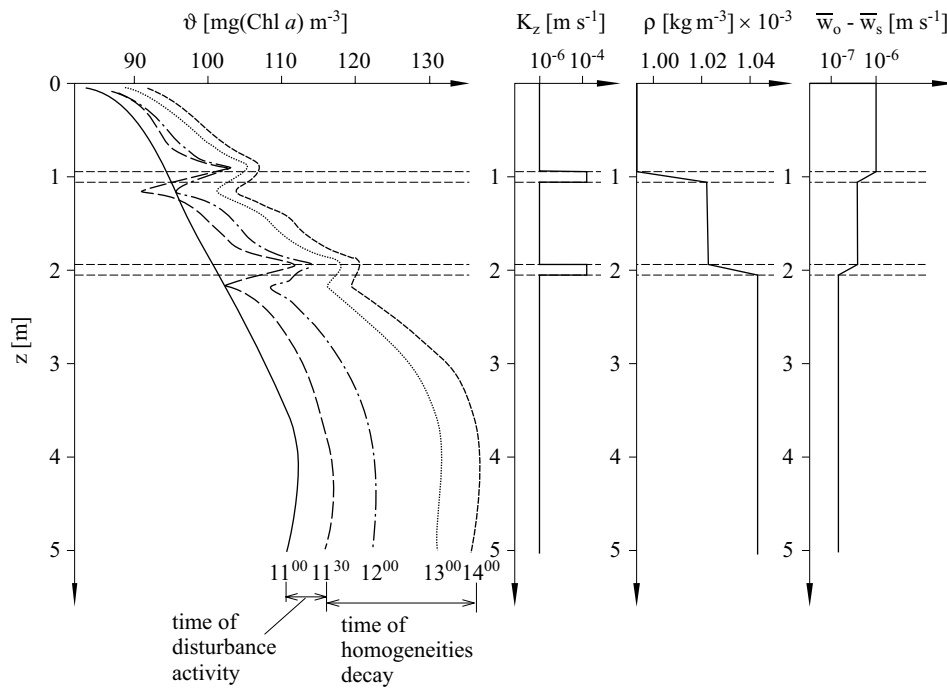


Fig. 24. Evolution in time of phytoplankton fine structure decay ϑ : results of numerical modelling (after Druet & Zieliński 1988)

processes of foraging, respiration and mortality were assumed to be linearly dependent on the concentration of phytoplankton. Photosynthesis was assumed to be the principal function of the source of phytoplankton production. Some results from these simulation studies are set out in Fig. 26. The intermittent structure of mixing processes in the $15 \geq 25$ m layer clearly distinguishes the turbulent layers, and the quasi-laminar interlayers formed after 15 minutes mixing make up the fine structure in the concentration field of phytoplankton and nutrients. After 60 minutes' mixing these structures begin to disappear. On the other hand, the steep vertical gradient of flow rates generating turbulent mixing throughout the water column causes the complete smoothing of inhomogeneities and the elimination of fine stratification in the phytoplankton concentration field. Under real conditions, therefore, clear evidence exists of the influence of intermittent fine structure dynamics in the concentration fields of both phytoplankton and nutrients. In these simulation studies the mean velocity \overline{w}_s was determined under the assumption that the vertical movement of phytoplankton is slow and that its velocity is close to the sinking speed of passive suspended matter in still, completely transparent water, as given by Stokes' formula:

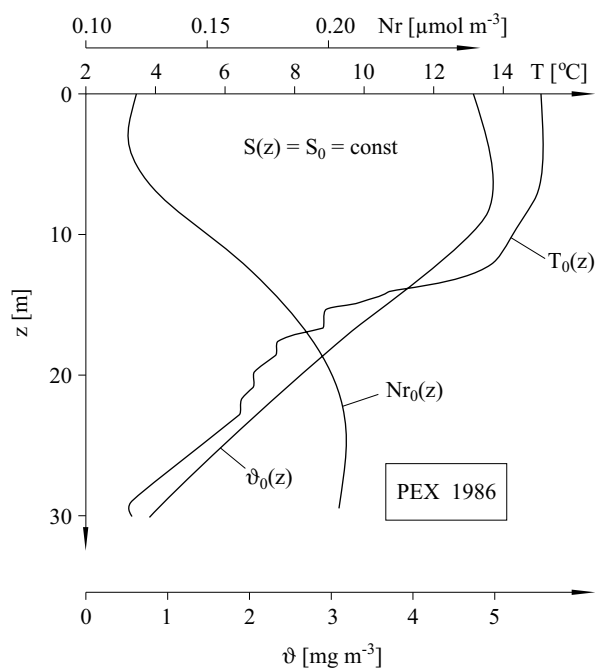


Fig. 25. Distribution of environmental properties: temperature T_0 , salinity S_0 , nutrients Nr_0 and chlorophyll concentration (ϑ_0) for a vertical gradient of current velocity $\partial \bar{u} / \partial z = 0$ (background data for the numerical modelling shown in Fig. 26)

$$\bar{w}_s(z) = \frac{g[\bar{\rho}_s - \bar{\rho}(z)]d^2}{18\mu}, \quad (36)$$

where $\bar{\rho}$ and $\bar{\rho}_s$ – water and suspension density in the unit volume, μ – dynamic coefficient of molecular viscosity, d – mean dimension of a suspended particle (for a phytoplankton cell $d \approx 10^{-6}$ m).

Stokes' formula is often used by researchers and yields satisfactory results in some modelling. But when fine structure exists, this is not a suitable formula. According to Lerman et al. (1977), the velocity \bar{w}_s , characterising the autonomous rise of phytoplankton, is of the order of 10^{-6} m s $^{-1}$. In 2002 the results of studies on the velocity \bar{w}_s by Huisman & Sommeijer (2002) were published. According to their data (see Fig. 27), the velocity depends on the degree of turbidity of the water, i.e. on local transparency conditions. So not only suspended mineral admixtures, but also the concentration of the phytoplankton itself hinder the movement of plant cells. This question remains an open one and requires further study, especially in view of the fact that Stokes' formula is inapplicable in conditions of turbulent mixing.

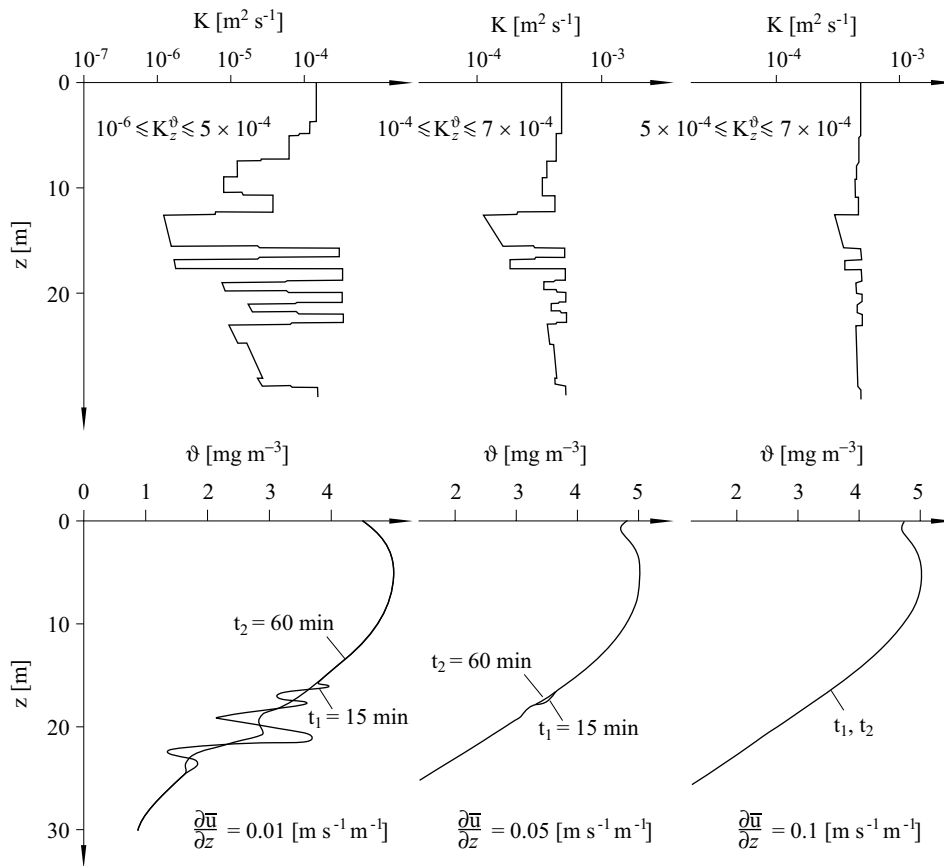


Fig. 26. Influence of turbulent mixing K_z^ϑ on the fine structure of chlorophyll *a* concentration along three constant gradients of shear velocity: $\partial\bar{u}/\partial z = 0.01 \text{ s}^{-1}$, $\partial\bar{u}/\partial z = 0.05 \text{ s}^{-1}$, $\partial\bar{u}/\partial z = 0.1 \text{ s}^{-1}$ (after Druet & Zieliński 1994)

The application of turbulent diffusion equations to the modelling of concentrations of herbivorous zooplankton, which in turn are fed upon by larval fish and carnivorous Copepoda, is a task more complex than the modelling of the hydrodynamically passive phytoplankton. Considering the minute sizes of this zooplankton, we can assume, without committing too serious an error, that turbulent mixing affects ambush-type microzooplankton in the same way as phytoplankton. However, when modelling zooplankton with a cruise-type behaviour, this assumption has to be rejected, because this zooplankton is capable of active movement. Its relations with a predator hunting for zooplanktonic prey are more complex and the foraging process as a component of the source function cannot be defined in the same way as that of phytoplankton, because the principal factor governing it is the

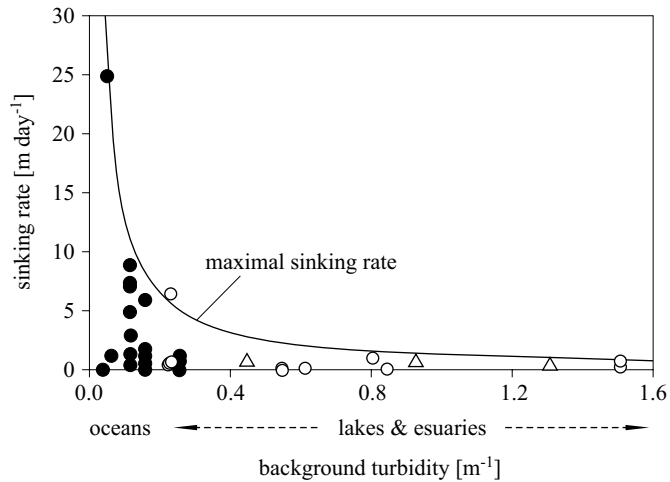


Fig. 27. Sinking velocity of phytoplankton species from oceans (\bullet), estuaries and rivers (Δ) and lakes (\circ), plotted as a function of background turbidity (after Huisman & Sommeijer 2002)

encounter rate between predator and prey. Merely by swimming about the prey animal produces certain acoustic signals which a predator can pick up while hunting. These signals are distorted by turbulent mixing to an extent that depends on the intensity of the turbulent motion. The power of the signal emitted by the prey animal is inversely proportional to the square of the distance from the predator. If the distance between the prey's cilia and the predator reduces to the 'reaction distance', then the predator begins to hunt. But turbulent mixing produces its own sound field which, because it is superimposed on the prey's acoustic field, will modify the signals received by the predator. So when turbulence is intense, the predator becomes 'deaf'. Moreover, a number of zooplankton species are capable of performing movements that produce a conical current by means of which they ingest food. When the flow of suspended plankton is sufficiently turbulent, the square of the orbital velocity of turbulent eddies w_{ω}^2 may be greater than the magnitude of $V_0 \frac{\nu}{d}$ (where V_0 is the velocity of the conical current, d is the size of the individual animal and ν is the coefficient of molecular viscosity) at a distance shorter than d . The zooplankton animal then becomes 'blind' and is incapable of feeding (Jimenez 1997).

It is clear, then, that turbulent mixing affects the behaviour of zooplankton both at rest and when it is actively in search of food. Considering that the speed of movement of prey items is a random variable in both time and space, its mean value is close to zero. If we assume that $\frac{\partial}{\partial z}(\bar{w}_s Q_p)$, the diffusion equations can be simplified to the following form:

$$\frac{\partial \bar{Q}_p}{\partial t} - \frac{\partial}{\partial z} \left[K(z) \frac{\partial \bar{Q}_p}{\partial z} \right] - \Pi_3 \bar{Q}_p - \Pi_4 = 0, \quad (37)$$

where Q_p is the prey concentration, and Π_3 is that part of the losses sustained by Q_p as a result of its physiological functions (ingestion, metabolic losses, egestion etc.) Π_4 represents the losses incurred by Q_p as a result of predation. Π_4 is the only component of the source function which is strongly dependent on the state of turbulent mixing, as has already been mentioned. Its magnitude can be determined from the biomass of the predator B on the assumption that the loss incurred by the prey concentration Q_p is proportional to the increase in the predator's biomass:

$$\Pi_4 = \alpha_2 B. \quad (38)$$

Hitherto, various values have been assigned to the proportionality coefficient α : many authors take $\alpha_2 \approx 0.1$. By contrast, the increase in predator biomass during foraging has been described in quite some detail in the literature. For example, an interesting approach was taken by Davis et al. (1991). They formulated the increase in biomass B thus:

$$\frac{\partial B}{\partial t} = m_B B + \frac{\partial^2}{\partial x^2} [K(x) + K_s(x)] B, \quad (39)$$

where the horizontal coordinate x is located along the mixed layer, m_B is the growth rate, and the coefficients $K(x)$ and $K_s(x)$ are the respective coefficients of physical diffusion and the predator's swimming diffusion.

The growth rate m_B and the coefficient of swimming diffusion K_s depend both on the magnitude of prey concentrations and on the encounter rate E_0 and can be expressed in the form (Davis et al. 1991):

$$m_B = m_1 E_0 + m_2, \quad K_s = n_1 E_0^{-1}, \quad (40)$$

where m_1 (prey⁻¹), m_2 (s⁻¹) and n_1 (m² s⁻²) are constant coefficients (prey \equiv the number of cells in individuals).

The encounter rate is governed by two kinds of processes – behavioural E_B , and hydrodynamic processes resulting from the interacting movements of water masses. The one condition emerges from the ability to perform autonomous movements (swimming). The other can be divided into the processes of floating and turbulent mixing. Neither predator nor prey experience floating as such. But turbulent mixing affects not only aggregation processes but also the speed of the predator's movement with respect to its prey. If we denote this influence by E_T , we can write: $E_0 = E_B + E_T$. The behavioural term E_B is usually taken to be that

proposed in the model by Gerritsen & Strickler (1977), under the assumption that the speed of the predator ν exceeds that of the prey u :

$$E_B = \pi \overline{Q}_p \ell^2 \left(\frac{u^2 + 3v^2}{3v} \right) \quad \text{for } v > u, \quad (41)$$

where ℓ is the distance between the centres of two touching spheres.

The other term E_T was expressed by Rothschild & Osborn (1988) in the form:

$$E_T = \pi \overline{Q}_p \ell^2 w_\omega, \quad (42)$$

where w_ω is the linear orbital velocity of turbulent eddies.

By substituting E_B and E_T to the E_0 equation Rothschild & Osborn (1988) obtained the formula

$$E_0 = \pi \overline{Q}_p \ell^2 \frac{u^2 + 3v^2 + 4w_\omega^2}{[3(v^2 + w_\omega^2)]^{1/2}}. \quad (43)$$

Evans (1989) analysed this formula in greater detail and suggested a somewhat different form of it:

$$E_0 = \pi \overline{Q}_p \ell^2 \frac{[u^2 + 3v^2 + 2w_\omega^2]^{1/2}}{[3(v^2 + w_\omega^2)]^{1/2}}. \quad (44)$$

The reasoning lying behind this representation of E_0 was based on the assumption that prey and predator move in straight lines along a section ℓ of concentration Q_p . Both, of course, move in a random fashion, and turbulent mixing, also a random process, makes its influence felt. In reality, therefore, E_0 is the resultant of a complex random process with respect to both E_B and E_T . For these reasons, then, the orbital velocity of turbulent eddies has come to be expressed as a mean square magnitude:

$$\left(\overline{w_\omega^2} \right)^{1/2} = \left\{ \overline{[\beta_0(\varepsilon \ell)^{1/3}]^2} \right\}^{1/2}, \quad (45)$$

where β_0 is a numerical coefficient of the order of unity. This expression indirectly takes the effect of the random nature of turbulent mixing on E_0 into consideration. However, the rather more sophisticated study by Seuront et al. (2001), based on a multifractal model, showed that the real effect of turbulent mixing on the value of E_0 is much less than that mentioned above, which does not allow for the intermittent nature of this process. According to these authors, the values of E_0 given by cited expressions are overestimated by around 30%.

Davis et al. (1991), in a study already mentioned here, presented the foraging process in an interesting light. Their model is based on three equations:

$$\left. \begin{aligned} \frac{\partial B}{\partial t} + \frac{\partial}{\partial x}(vB_r) &= 0, \\ \frac{\partial B}{\partial t} + \frac{\partial}{\partial x}[v(B - b_{re})] + (2n_T + n_s)B &= 0, \\ \frac{\partial b_{re}}{\partial t} + n_s B + (n_s + n_r)b_{re} &= 0, \end{aligned} \right\} \quad (46)$$

where $B_r = b_r - b_\ell$, b_r is the biomass of a predator moving to the right, b_ℓ is the mass of a predator moving to the left, and b_{re} is the mass of a predator at rest. n_s is the number of times the predator stops moving, n_R is the number of times the predator starts moving (the rate of starting), and n_T is the number of times the predator turns without stopping (the rate of turning). The x axis is aligned along the direction of movement of the predator.

The system of these equations has a stable solution when $B_r = 0$ and $v(B - b_{re}) = \text{const}$, so long as B , B_r and b_{re} are constant in time. Taking this into account, we obtain the following form:

$$B = \frac{n_s + n_R}{v n_R} = \text{const}. \quad (47)$$

This expression demonstrates incontrovertibly that a predator will forage wherever the prey concentration is greatest, because in such an area the value of n_s is at a maximum and that of n_R at a minimum – the predator is then usually stationary and changes its position as little as possible. The low speed of the predator ν lends further support to this idea. If we assume that the time taken for a predator to move through an aggregation of prey is much longer than the starting time (n_R^{-1}), the standstill time (n_s^{-1}) and the turning time (n_T^{-1}), we can then also assume that the last two equations in this system will always be in a state close to equilibrium. Then:

$$b_{re} = \frac{n_s}{n_s + n_R} B \quad \text{and} \quad B_r = -\frac{1}{2n_T + n_s} \frac{\partial}{\partial x} \left(\frac{v n_R}{n_s + n_R} B \right), \quad (48)$$

and the increase in biomass will proceed in accordance with the formula

$$\frac{\partial B}{\partial t} = \frac{\partial}{\partial x} \left[\left(\frac{v}{2n_T + n_s} \right) \frac{\partial}{\partial x} \left(\frac{v n_R}{n_s + n_R} \right) B \right]. \quad (49)$$

This equation can also be written in the form (Davis et al. 1991):

$$\frac{\partial B}{\partial t} = \frac{\partial}{\partial x} k_1 B \frac{\partial}{\partial x} k_2 B. \quad (50)$$

Both of above equations are equivalent when coefficients k_1 and k_2 are equal to:

$$k_1 = \frac{v}{2n_T + n_s} \quad \text{and} \quad k_2 = \frac{v n_R}{n_s + n_R}. \quad (51)$$

It is evident from the above that in an area of high prey concentration, a predator is more likely to remain stationary than swim around. Furthermore, if more time is spent being stationary, then less will be available for turning without stopping. Therefore, n_T and n_R decrease while n_s increases. All this goes to show that the predator remains in an area of high concentration not because it has a memory but because it spends more time feeding than hunting.

From this theory Davis et al. (1991) obtained results, some of which are reproduced on Fig. 28, which demonstrate conclusively that turbulent mixing exerts a considerable influence on a predator's growth rate. Further evidence is provided by the results of a study by MacKenzie et al. (1994) on the effect of turbulence on the encounter rate (A), the probability of successful pursuit (B) and the ingestion rate (C), as shown on Fig. 29. These plots show clearly that the stronger the turbulent mixing, the less likely is a successful hunt and the lower the foraging rate by larval fish even when the encounter rate simultaneously rises. As the turbulence increases, the larval fish is compelled to intensify its movements in order to capture prey from an ever-decreasing aggregation.

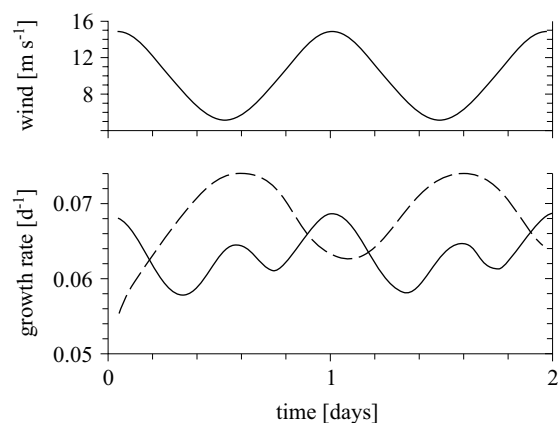


Fig. 28. Effects of temporarily varying winds (top panel) on plankton growth at the upper (solid line) and lower (dashed line) boundary of the 10-metre thick mixed surface layer (after Davis et al. 1991)

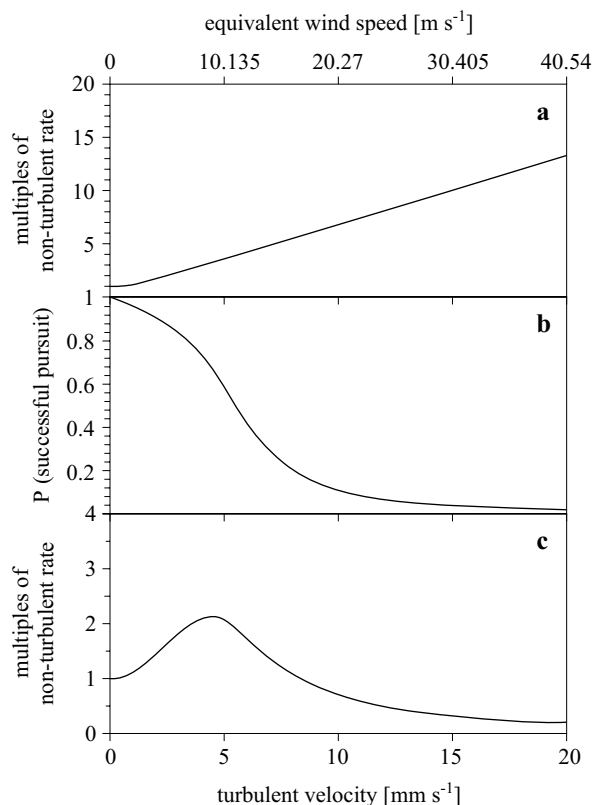


Fig. 29. The influence of turbulent mixing on: a – encounter rate, b – probability of successful pursuit, c – relative ingestion rate for larval cod (after McKenzie et al. 1994)

Let us now move on to consider the effect of fine structure on the concentration field of herbivorous zooplankton Q_p foraged upon by carnivorous zooplankton. Assuming that in the vertical fine structure the mixed and gradiental layers are horizontally homogeneous over far greater distances than a predator's instantaneous hunting area, and that over these horizontal distances the prey concentration is constant, varying only in the vertical, we can write the diffusion equation in the form:

$$\frac{\partial \bar{Q}_p(z, t)}{\partial t} - \frac{\partial}{\partial z} \left[K(z) \frac{\partial \bar{Q}_p(z, t)}{\partial z} \right] - \Pi_3 \bar{Q}_p(z, t) - \alpha_2 \bar{B}(z, t) = 0. \quad (52)$$

We can carry out time-space simulations of the vertical variability of concentrations \bar{Q}_p in fine structure layers on the basis of this equation. To do this, we need to define the appropriate initial and boundary conditions at the upper (i.e. free surface) and lower (i.e. euphotic zone boundary)

boundaries of the basin. In fact, these conditions can be defined for any levels, wherever the values of \overline{B} and \overline{Q}_p are known for a given starting point. The area usually considered in the literature is the upper, homogeneous, completely mixed layer of the sea, where it is a relatively straightforward matter to define both the behavioural and hydrodynamic parameters of the process to be simulated. However, the problem of the turbulent diffusion of plankton in the fine structure area, which is addressed in this article, remains an open research question, and the few attempts undertaken so far to resolve it are still far from achieving a satisfactory practical effect.

4. Conclusions

1. To put the matter in a nutshell, we are still a long way from being able to provide a reliable description of intermittent fine structure itself and its dynamic transformations, as well as of the effect of these processes on the behaviour of marine plankton. The empirical work, both *in situ* and laboratory experimentation, as well as mathematical modelling, though having reached quite an advanced stage, must therefore be continued.
2. In a gravitationally absolutely stable basin, the fine structure is created by the inertial instability of horizontal flows of water at different depths. The turbulent mixing that occurs in such intermittent stratification homogenises the plankton contained in destabilised layers. The turbulent diffusion processes accompanying homogenisation thin out the aggregations of suspended matter and, depending on the direction of vertical transfer (downwelling or upwelling), they increase the concentration of plankton in the vicinity of laminar or quasi-laminar thin interlayers, which are characterised by steep vertical gradients of the physical properties of water. In conditions such as these, an elevated concentration of phytoplankton and ambush-type zooplankton near the laminar interlayers will also cause larger numbers of foraging cruise-type predators to move to this area, since they prefer to feed when stationary rather than actively swimming about. This fact thus identifies the depth levels where larval fish forage in the fine structure area of the euphotic zone.
3. In conditions where the relative gravitational stability of the water masses is due to a thermal inversion, the fine structure is generated by the intermittent intrusion of foreign water masses differing in temperature and salinity from the surroundings. Where these intrusions impinge on the surrounding waters, laminar convection cells are formed which, once the critical Rayleigh number has been

exceeded, are subject to gravitational destabilisation, which in turn gives rise to a turbulent mixed layer along the entire length of the intrusion. Given these conditions, planktonic aggregations of prey will be subject to homogenisation during laminar and turbulent mixing, a process which will continue until the thermal inhomogeneities have levelled out. It is therefore to be expected that this kind of intermittent fine structure localisation of a predator's foraging area will depend on the variability of prey concentration within the mixed cloud. Where this concentration is greater, we can expect larger aggregations of predators. However, the present state of knowledge does not allow us to point to a particular area of elevated prey concentration. Very probably, such areas will be randomly variable in time and that the predator will be forced to swim around continually.

4. In conditions where the relative gravitational stability is due to a salinity inversion, the mixed layer is formed by salt fingers. The vertical movement of water – upwards in 'convection channels' and downwards in saline 'gravitational channels' – is laminar. Thus in layers that are as thick as the salt fingers are long, homogenisation of plankton will occur by slow molecular diffusion, and its degree of concentration will depend both on the species of plankton and on the duration of the salt finger structure. But the almost total lack of research communications on the relationship between this kind of fine structure and the effects of plankton diffusion occurring there preclude any further meaningful discussion of this subject.

References

- Axell L.B., 2002, *Wind-driven internal waves and Langmuir circulations in numerical ocean model of the Southern Baltic Sea*, J. Geophys. Res., 107 (C11), 1–19.
- Baumert H., Peters H., 2000, *Second-moment closures and length scales for weakly stratified turbulent shear flows*, J. Geophys. Res., 105 (C3), 6453–6468.
- Davis C.S., Flierl G.R., Wiebe P.H., Franks P.J.S., 1991, *Micropatchiness, turbulence and recruitment in plankton*, J. Mar. Res., 49 (1), 109–151.
- Dillon T.M., 1982, *Vertical overturns: a comparison of Thorpe and Ozmidov length scale*, J. Geophys. Res., 87 (C12), 9601–9613.
- Dower J.F., Miller Th.J., Leggett W.C., 1997, *The role of microscale turbulence in the feeding of larval fish*, Adv. Mar. Biol., 31, 170–220.
- Druet C., Siwecki R., 1983, *The fine structure of hydrophysical fields in the sea Kamchiya Experiment 1977*, Stud. i Mater. Oceanol., 40, 259–288, (in Polish).

- Druet C., Siwecki R., 1984, *On the usefulness of the Cox number in investigations on the intensity of turbulent heat exchange processes in the coastal zone*, Oceanologia, 18, 37–49.
- Druet C., Siwecki R., 1985, *Small-scale stratification of the density field and its influence on the suspensions' concentration*, Oceanologia, 21, 33–57.
- Druet C., Siwecki A., 1993, *Vertical fine structure and small-scale mixing in the upper ocean layer of the Norwegian-Barents confluence zone*, Stud. i Mater. Oceanol., 65 (2), 150–169.
- Druet C., Zieliński A., 1988, *The effect of dynamic properties of a vertically stratified sea and biogenic factors on the concentration of phytoplankton*, Oceanologia, 26, 63–79.
- Druet Z., Zieliński A., 1994, *Modelling the fine-structure of the phytoplankton concentration in a stable stratified sea*, Oceanol. Acta, 17(1), 79–88.
- Dzierzbicka-Głowacka L., 2000, *Mathematical modelling of the biological processes in the upper layer of the sea*, Rozpr. i monogr., Inst. Oceanol. PAN, Sopot, 13, 123 pp., (in Polish).
- Evans G. T., 1989, *The encounter speed of moving predator and prey*, J. Plankton Res., 11, 415–417.
- Gargett A. E., 1978, *Microstructure and fine structure in an upper ocean frontal regime*, J. Geophys. Res., 83 (C10), 5123–5134.
- Gargett A. E., 1997, *Theories and techniques for observing turbulence in the ocean euphotic zone*, [in:] *Lecture notes on plankton and turbulence*, C. Marrasé, E. Saiz & J. M. Redondo (eds.), Sc. Marina, 61, Suppl. 1, 25–45.
- Gargett A. E., Osborn T. R., Nasmyth P. W., 1984, *Local isotropy and the decay of turbulence in a stratified fluid*, J. Fluid Mech., 144, 231–280.
- Gargett A. E., Schmitt R. W., 1982, *Observations of salt fingers in the central waters of the eastern North Pacific*, J. Geophys. Res., 87 (C10), 8017–8029.
- Garrett C., Munk W., 1972, *Oceanic mixing by breaking internal waves*, Deep-Sea Res., 19 (12), 823–832.
- Gerritsen J., Strickler J. R., 1977, *Encounter probabilities and community structure in zooplankton: a mathematical model*, J. Fish Res. Bd Can., 34, 73–82.
- Gibson C. H., 1987, *Fossil turbulence and intermittency in sampling oceanic mixing process*, J. Geophys. Res., 92 (C5), 5383–5404.
- Gregg M. C., 1989, *Scaling turbulent dissipation in the thermohaline*, J. Geophys. Res., 94 (C7), 9684–9698.
- Huisman J., Sommeijer B., 2002, *Maximal sustainable sinking velocity of phytoplankton*, Mar. Ecol. Prog. Ser., 244, 39–48.
- Icha A., Siwecki R., 1988, *New approach to Cox Number in quasi-homogeneous layer*, Proc. Liege Coll. No. 46, pp. 35–36; *Small-scale turbulence and mixing in the ocean*, J. C. J. Nihoul & B. M. Jamart (eds.), Elsevier, Amsterdam.
- Itsweire E. C., Koseff J. R., Briggs D. A., Ferziger J. H., 1993, *Turbulence in stratified shear flows*, J. Phys. Oceanogr., 23 (7), 1508–1522.

- Ivey G.N., Imberger J., 1991, *On the nature of turbulence in a stratified fluid, part 1: the energetics of mixing*, J. Phys. Oceanogr., 21 (5), 650–658.
- Jimenez J., 1997, *Oceanic turbulence at millimeter scales*, Sc. Marina, 61, Suppl. 1, 49–56.
- Kjørboe T., Saize E., 1995, *Planktivorous feeding in calm and turbulent environments with emphasis on copepods*, Mar. Ecol. Prog. Ser., 122, 135–145.
- Kolmogorov A.N., 1962, *A refinement of previous hypotheses concerning the local structure of turbulence in a viscous incompressible fluid at high Reynolds number*, J. Fluid Mech., 13 (1), 82–85.
- Large W.G., Gent P.R., 1999, *Validation of vertical mixing in an equatorial ocean model, using large eddy simulations and observations*, J. Phys. Oceanogr., 29 (3), 449–452.
- Lehfeldt R., Bloss S., 1988, *Algebraic turbulence model for stratified tidal flows*, [in:] *Physical processes in estuaries*, J. Dronkers & W. Leussen van (eds.), Springer Verl., 278–291.
- Lerman A., Carder K.L., Betzer P.R., 1977, *Elimination of fine suspended soil in the oceanic water column*, Earth Plan. Sci. Lett., 37 (1), 61–71.
- Lubimtzev M.M., 1985, *Model of interaction of intermittent turbulence and fine structure of oceanic hydrophysical fields*, Okeanologiya, 25 (6), 903–910, (in Russian).
- MacKenzie B.R., Kjørboe T., 2000, *Larval fish feeding and turbulence*, Limnol. Oceanogr., 45 (1), 1–8.
- MacKenzie B.R., Miller T.J., Cyr S., Leggett W.C., 1994, *Evidence of a dome – shaped relationship between turbulence and larval fish ingestion's rates*, Limnol. Oceanogr., 39, 1790–1799.
- Marmorino G.O., Brwon W.K., Moriiis W.D., 1987, *Two-dimensional temperature structure in the C-SALT thermohaline staircase*, Deep-Sea Res., 34 (10), 1667–1676.
- McDougall T.J., Thorpe S.A., Gibson C.H., 1988, *Small-scale turbulence and mixing in the ocean: a glossary*, Proc Liege Coll. No. 46, pp. 3–9; *Small-scale turbulence and mixing in the ocean*, J.C.J. Nihoul & B.M. Jamart (eds.), Elsevier, Amsterdam.
- Monin A.S., Ozmidov R.V., 1981, *Oceanic turbulence*, Gidrometeoizdat, Leningrad, 320 pp., (in Russian).
- Munk W.H., Anderson E.R., 1948, *Notes on a theory of the thermocline*, J. Mar. Res., 7 (3), 275–295.
- Nunes Vaz R.A., Simpson J.H., 1994, *Turbulence closure modelling of estuarine stratification*, J. Geophys. Res., 99 (C8), 16143–16160.
- Osborn T.R., 1980, *Estimates of the local rate of vertical diffusion from dissipation measurements*, J. Phys. Oceanogr., 10 (1), 83–89.
- Osborn T.R., Cox C.S., 1972, *Oceanic fine structure*, Geophys. Fluid Dyn., 3, 321–345.

- Ozmidov R. V., 1965, *Turbulent exchange in the stably stratified ocean*, Izv. Akad. Nauk SSSR – Fiz. Atmos. Okeana, 1 (8), 853–860, (in Russian).
- Ozmidov R. V., 1983, *Small-scale turbulence and fine structure of hydro-physical fields in the ocean*, Okeanologiya, 23 (4), 533–537, (in Russian).
- Pacanowski R. C., Philander S. G. H., 1981, *Parametrization of vertical mixing in numerical models of tropical ocean*, J. Phys. Oceanogr., 11, 1443–1451.
- Peters H., Gregg M. C., Toole J. M., 1988, *On the parametrization of equatorial turbulence*, J. Geophys. Res., 93 (C2), 1199–1218.
- Peters F., Marrase C., 2000, *Effects of turbulence on plankton; an overview of experimental evidence and some theoretical considerations*, Mar. Ecol. Prog. Ser., 205, 291–306.
- Rothschild B. J., Osborn T. R., 1988, *Small-scale turbulence and plankton contact rates*, J. Plankton Res., 10, 465–474.
- Schmitt R. W., 1979, *The growth rate of supercritical salt fingers*, Deep-Sea Res., 26 (1A), 23–40.
- Seuront L., Schmitt F., Lagadene Y., 2001, *Turbulent intermittency, small-scale phytoplankton patchiness and encounter rates in plankton: where do we go from here?*, Deep-Sea Res., 48, 1199–1215.
- Stern M. E., 1975, *Ocean circulation physics*, Int. Geophys. Ser., 19, Acad. Press., New York, 246 pp.
- Thorpe S. A., 1977, *Turbulence and mixing in the Scottish Loch*, Phill. Trans. Roy. Soc., 286, 125–181.
- Turner L. S., 1973, *Buoyancy effects in fluid*, Cambridge Univ. Press., London, 367 pp.
- Van Atta C. W., 1998, *A generalised Osborn Cox model for estimating fluxes in nonequilibrium stably stratified turbulent shear flow*, J. Mar. Sys., 21 (1)–(4), 103–110.
- Yamazaki H., Squires K. D., 1996, *Comparison of oceanic turbulence and copepod swimming*, Mar. Ecol. Prog. Ser., 144, 299–301.
- Žurbas W. M., Lips U. K., 1987, *Method and classification of fine thermohaline structure in the ocean, Part 1.2*, [in:] *Principals of fine-structure and methodes of its description*, Geophys. Comm. Acad. Sci. USSR, Moscow, 15–22, (in Russian).